Engineering of *Corynebacterium glutamicum*

For the Secretion of Lignin-modifying Enzymes

by

Dylan Ellis

A Thesis Presented in Partial Fulfillment
of the Requirements for the Degree
Master of Science

Approved March 2022 by the
Graduate Supervisory Committee:

Arul Mozhy Varman, Chair
Peter Lammers
Timothy Long

ARIZONA STATE UNIVERSITY

May 2022

ABSTRACT

Lignin is a naturally abundant source of aromatic carbon but is largely underutilized in industry because it is difficult to decompose. Recent research activity has targeted the development of a biological platform for the conversion of lignin and lignin-derived feedstock. *Corynebacterium glutamicum* is a standout candidate for the bacterial depolymerization and assimilation of lignin because of its performance as an industrial producer of amino acids, resistance to aromatic compounds in lignin, and low extracellular protease activity. Under the current study, nine experimental strains of *C. glutamicum* were engineered with sequencing-confirmed plasmids to overexpress and secrete lignin-modifying enzymes with the eventual goal of using lignin as raw feed for the sustainable production of valuable chemicals. Within the study, laccase and peroxidase activity were discovered to be decreased in *C. glutamicum* culture media. For laccase the decrease reached statistical significance, with an activity of about 10.9 U/L observed in water but only about 7.56 U/L and 7.42 U/L in fresh and spent BHI media, respectively, despite the same amounts of enzyme being added. Hypothesized reasons for this inhibitory effect are discussed here, but further work is needed to identify causative factors and realize the potential of *C. glutamicum* for waste biomass valorization.

ACKNOWLEDGMENTS

There are many people I would love to thank for their support in my project and throughout my time at Arizona State. First and foremost, thank you Dr. Arul Varman for your advising, kindness, and, and investment in my growth – I have learned so much from you and am so glad to have been a member of the lab. Thank you Arren Liu, Apurv Mhatre, and Dr. Aditya Sarnaik for your encouragement and enthusiastic mentorship. Thank you Amogh Deshpande for help in experiments and being my first research mentee. Thank you to my lab mates Nima Hajinajaf, Danika Kartchner, Jason Ronstadt, Andrew Reed, William Ederer, Tyler OKane, Parker Poole, Haley McKeown, Bethany Kalscheur, Muhammad Faisal, Abigail Jansen, Kira Winsor, Carlie Rein, and Elissa Balbas for making our lab feel like a home and for inspiring me to always do and be my best. Thank you to Dr. Peter Lammers and Dr. Timothy Long for your support on my thesis committee.

Outside of this lab, thank you to Dr. Gregor Kosec, Dr. Martin Kavšček, and my lab mates from Acies Bio for sparking my interest in synthetic biology, and to Dr. Noa Rappaport, Dr. Priyanka Baloni, Dr. Cory Funk, and my lab mates at the Institute for Systems Biology for all the opportunities to grow as a researcher and expand my skills. Thank you to my family and friends for all your love support throughout my journey thus far – I could not have done it without you.

Finally, thank you to Barrett, the Honors College and the Fulton Schools of Engineering Fulton Undergraduate Research Initiative (FURI) and Master's Opportunity for Research in Engineering (MORE) for funding this project.

TABLE OF CONTENTS

Page

LIST OF TABLES

LIST OF FIGURES

Figure Page

LIST OF SYMBOLS

Symbol Page

CHAPTER 1

INTRODUCTION

Lignin, its depolymerization, and prior work

Lignin, along with cellulose and hemicellulose, is one of the three components of lignocellulose[1]. Because biomass is an abundant and renewable resource, valorization of lignocellulose has been a goal of significant interest. Recently, cellulose and hemicellulose have been the primary focus for the valorization of plant biomass, a 'sugar-based platform,' because lignin is particularly recalcitrant due to its complex structure[1]. Left untreated, lignin becomes a pollutant due to its recalcitrance and volume of production: in the US alone, over 62 million tons of lignin waste are produced annually[2]. Because it is hard to break down, 98% of industrial lignin is only burned for fuel and thus underutilized[1].

However, lignin valorization is incredibly attractive and desired because of availability and chemical composition. With over 300 billion tons of lignin available on earth and steadily increasing, lignin is the most abundant source of aromatic carbon[1,2]. Aromatic carbon is a vital component to many different valuable products such as pharmaceuticals, biofuels, and cosmetics. By enabling the use of the phenolics derived from lignin, waste would be diverted and a more cost-effective and sustainable feed for value-added compounds would be generated. Current technologies for lignin valorization include thermochemical methods such as hydrogenolysis, hydrothermal liquefaction, hydrothermal carbonization, cracking, and various other catalytic techniques[2]. These technologies allow for monolignins to be efficiently recovered and used for value-added products, but also require the use high temperatures and the release of harmful pollutants

and chemicals[2]. Lignin degradation and subsequent valorization via biorefinery would be a 'greener' alternative to enhance sustainable production by converting lignin waste to valuable raw material with little to no harmful byproducts[2].

Natural lignin degradation has been most studied in white and brown-rot fungi, but many bacteria have been found also be vital contributors to its breakdown, such as *Streptomyces, Rhodococcus, Pseudomonas,* and *Bacillus*[2,3]. These organisms depolymerize lignin by producing various ligninolytic enzymes, specifically peroxidases and laccases[1]. The ligninolytic class II peroxidases can be mostly broken into the categories of lignin peroxidases, manganese peroxidases, and versatile peroxidases (VPs)[1]. Each of these peroxidases require hydrogen peroxide to generate radical mediators to cleave recalcitrant lignin bonds, and mostly occur in fungi[2]. Another class of peroxidases important specifically to bacterial lignin degradation are dye-decolorizing peroxidases, which are more common in bacteria than fungi[3]. Laccases, a type of blue multi-copper oxidase, on the other hand are common in both fungi and bacteria, as well as plants and insects[4]. Laccases do not require hydrogen peroxide (instead using molecular oxygen) or cofactors to depolymerize lignin and do not generate toxic peroxide intermediates, unlike peroxidases[4]. However, laccases also typically only cleave phenolic units of lignin, as they have a lower redox potential than peroxidases[2]. Other accessory enzymes engaging in lignin degradation include β-etherases, O-demethylases, and select carboxylases[1].

A leading approach to the valorization of lignin is through engineering organisms to depolymerize lignin and assimilate the degradation products into their metabolism. Prior work toward the first goal of depolymerization includes the development of a strain

of baker's yeast *Saccharomyces cerevisiae* containing a full ligninolytic secretome[5]. The strain included an evolved laccase originally derived from *Trametes trogii*, LacChuB, and an evolved VP originally derived from *Pleurotus eryngii*, PO21B, which are both top performing ligninolytic enzymes[6,7]. The enzyme kinetic data for PM1 Laccase (OB-1 mutant), an ancestor to the laboratory-evolved LacChuB laccase, is given in **Table 1**[8]. However, fungal expression hosts are more difficult to work with than bacteria. So far, a robust bacterial strain capable of degrading lignin in a biorefinery at industrial scale has not been achieved. For a bacterial strain to be effective, the heterologous expression of hydrolyzing enzymes of fungal origin is required. This creates a challenge as there are many differences in expressing proteins between eukaryotes and prokaryotes. Gonzalez-Perez and Alcalde describe protein misfolding difficulties because of differences in codon usage, post-translation modification, and chaperone proteins[5]. Another challenge of depolymerizing and assimilating lignin with engineered bacteria is the toxicity of the aromatic/phenolic compounds produced.

C. glutamicum as a platform for lignin valorization

Corynebacterium glutamicum is one top candidate bacteria proposed for the degradation of lignin. The soil bacterium has been commercialized with a long history of success for the industrial production of amino acids and has many favorable characteristics for the degradation and utilization of lignin. Shen et al. describes that while the growth and production of most bacteria are severely limited by lignin-derived phenolic compounds, *C. glutamicum* can withstand inhibitions associated with use of a lignocellulosic feed[9]. Compared to other organisms, *C. glutamicum* exhibits excellent performance in the degradation, assimilation, transport, and regulation of aromatic

compounds, utilizing them directly in central metabolic pathways[9]. One study by Becker et al. proved the potential of *C. glutamicum* for the valorization of lignin by producing *cis, cis*-muconic acid at high levels directly from lignin hydrolysates[10].

Other advantages of *C. glutamicum* include being gram positive, non-pathogenic, able to grow at facultatively anaerobic conditions, and malleable to metabolic engineering[11,12]. *C. glutamicum* also has many characteristics specifically addressing the challenge of expressing heterologous fungal enzymes. For one, *C. glutamicum* exhibits low extracellular protease activity, preventing secreted proteins from being degraded[11,13]. Having less proteins in the extracellular fluid in general also simplifies target protein purification[13]. Furthermore, the oxidative supernatant is conducive to proper protein folding and expression[13]. Finally, *C. glutamicum* does not require cell disruption to obtain proteins[13].

The *C. glutamicum* ATCC 13032 genome also exhibits its own endogenous laccase, CgL1, capable of degrading lignin[14]. Based on alignments using the National Center for Biotechnology Information (NCBI) Protein Basic Local Alignment Search Tool (BLASTp), the PM1 Laccase (OB-1 mutant) ancestor to LacChuB and CgL1 showed significant similarity in amino acid sequence[15]. To further support homology between the enzymes beyond amino acid sequence alone, the UniProt Knowledgebase shows both to contain three similarly spaced plastocyanin-like domains[16]. The *in vitro* reaction properties for the endogenous CgL1 laccase and the laboratory-evolved PM1 Laccase (OB-1 mutant) for ABTS substrate are compared in **Table 1**.

Table 1. Comparison of endogenous *C. glutamicum* CgL1 laccase (Ricklefs et al.) and laboratory-evolved PM1 Laccase (Maté et al.). *Data for both enzymes were obtained from in vitro studies with ABTS as substrate. The evolved laccase shows activity magnitudes greater than the endogenous laccase. Utilizing the evolved, heterologous laccase in a modified C. glutamicum system may decrease this high efficacy due to differences in protein folding and extracellular transport.*

Enzyme Property	*C. glutamicum* CgL1 Laccase[14]	Evolved PM1 Laccase (data from OB-1 mutant, ancestor to LacChuB)[8]
Optimal Temperature	60 ^{o}C	80 ^{o}C
Optimal pH	7.0	3.0
Michaelis-Menten Constant, K_M	2.2 mM	0.0063 mM
Catalytic Rate Constant k_{cat}	1.61 sec^{-1}	~ 200 sec^{-1}

Based on the observed enzyme kinetics, the PM1 Laccase substantially outperforms the CgL1 laccase *in vitro* in both turnover rate and binding affinity. However, it is worth testing both in this study because the difference in cellular machinery in *C. glutamicum* could render the heterologous enzyme less effective. The fungal enzymes may require post-translational modifications or specific chaperones to fold properly, unavailable in a prokaryotic host. The temperature and pH optima of the enzymes are also important considerations because they greatly impact protein folding, enzymatic activity, and cell growth. *C. glutamicum* grows optimally at 30 ^{o}C, and is able to grow at pH between 5.5-9.0 (having an internal pH of 7.5 +/- 0.5)[17]. Both the LacChuB and PO21B enzymes used in this study were developed via directed evolution to overcome some of the hurdles involved with utilizing fungal enzymes in a broader range of common environments, including improving activity in more alkaline conditions, which are required for model bacterial growth[6,7].

One plasmid suitable for the expression of ligninolytic enzymes in *C. glutamicum* is *pCRB204*. *pCRB204* is a protein shuttle vector designed by Okino et al. to produce D-lactic acid. It contains both an *Escherichia coli* and *Corynebacterium* origin of replication as well as a chloramphenicol (Cm) resistance gene. *pCRB204*'s promoter is *C. glutamicum* L-lactate dehydrogenase A promoter, which is induced via oxygen deprivation. While *pCRB204* also contains a *Lactobacillus delbrueckii* D-lactate dehydrogenase A gene (*ldhA*), it would be substituted with another gene for the desired protein to be expressed and secreted. The *C. glutamicum* strain with *pCRB204* plasmid showed five times higher productivity of D-lactate dehydrogenase A than the original strain at the beginning of the study[18].

Signal peptides as a secretion mechanism

C. glutamicum exhibits two main pathways for protein secretion, depicted in **Figure 1**: the secretory (SEC) pathway, and the twin-arginine translocation (TAT) pathway. Both pathways utilize signal peptides (SPs) attached to the target protein. Cellular machinery recognizes and binds to specific SPs to secrete the protein to the extracellular space. During secretion, the SP is cleaved by a signal peptidase (SPase). In the SEC pathway, proteins are exported while unfolded. In the cell, the peptides can be targeted in either a co-translational or post-translational mode. The SEC pathway is the most common pathway. On the other hand, the TAT pathway exports proteins already folded in the cell. The proteins docks to one complex and is translocated through another pore complex. The TAT pathway derives its name from the highly conserved "twin arginine" amino acids in the SP[11,13]. Bacterial laccases commonly exhibit TAT pathway SPs[4].

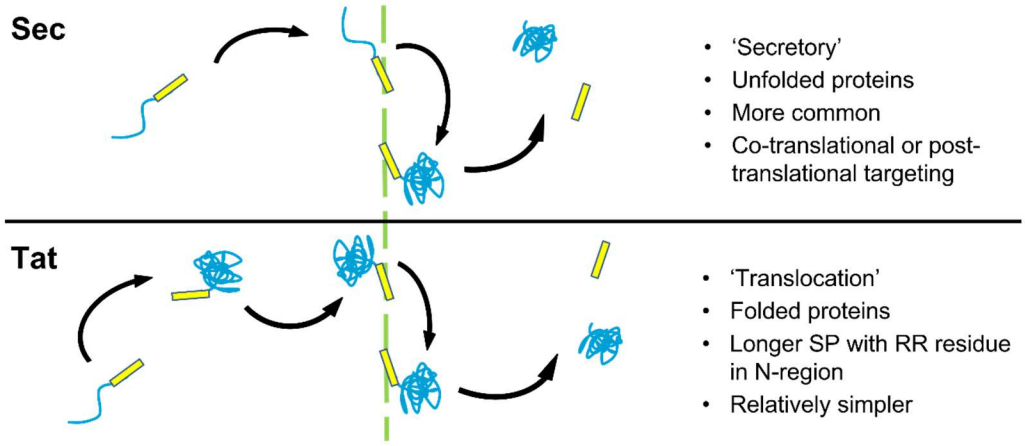

Figure 1: Depiction of protein secretion mechanisms via SPs in *C. glutamicum*. *Two main pathways exist, depending on where the protein folds: the secretory (SEC) pathway for extracellular folding, and twin-arginine translocation (TAT) pathway for intracellular folding (figure inspired by Lee & Kim*[13]*).*

Interactions between host cell machinery, enzyme, and SP significantly impact protein secretion and expression – one effective SP for one protein may not be as effective for a different protein, and an effective combination may not work in another organism. Currently, there is no robust method for predicting host/protein/SP combination efficacies. Therefore, according to Hemmerich et al., each new combination of production host, protein, and SP must be analyzed from scratch[19]. A step even further, Rohe et al. explains that with each of these new combinations, bioprocess parameters such as media and induction strategy must be re-optimized[20]. Hence, it is important to investigate many different organism/protein/SP combinations.

There are many candidate SPs for a *C. glutamicum* secretion system. For one, a 37 amino acid long TAT pathway SP is attributed the aforementioned CgL1 laccase endogenous to *C. glutamicum* (termed in this study as CgL1SP)[14]. Watanabe et al. performed a study screening all SPs in *C. glutamicum* R and testing their performance for the secretion of *Geobacillus stearothermophilus* α-amylase. In the study, 405 candidate

SPs were identified, 108 of which were able to secrete α-amylase. One TAT pathway SP, CgR0949, showed the greatest activity of all SPs, and an activity 150 times that of PS2, the most common secretory protein in *C. glutamicum*[21]. In another study, CgR0949 was the top-performing SP for the secretion of xylosidase by *C. glutamicum* ATCC 13032[22].

C. glutamicum has also been shown to effectively utilize heterologous SPs. Hemmerich et al. used *Bacillus subtilis* SEC pathway SPs in *C. glutamicum* for the secretion of cutinase, a eukaryotic protein[19]. One of the SPs utilized was YwmC, the top-performing SP in the full genome sweep of *B. subtilis* by Brockmeier et al. for the secretion of the metagenomic esterase EstCL1 by *B. subtilis*[23]. In the study by Hemmerich et al., utilizing the YwmC SP for the secretion of cutinase by *C. glutamicum* showed an increase in both absolute and relative activity from those obtained when using *B. subtilis* as a host[19]. When utilizing heterologous SPs, one important consideration is the cleavage site. Specific cleavage site sequences of SPs are recognized by SPases unique to the host cell. The genome-wide study of *C. glutamicum* R SPs performed by Watanabe et al. suggests the recognized cleavage site for *C. glutamicum* SPs in both the SEC and TAT pathways may consist of alanine residues at the -3 and -1 positions, and the secretion efficiency may be enhanced by a glutamine residue at the +1 position[21]. Using a cleavage site compatible with the host organism is important to ensure SPase recognition and the cleavage of the SP to allow for proper protein folding and function.

Study design

In this study, strains of *C. glutamicum* ATCC 13032 were engineered to secrete CgL1 laccase from *C. glutamicum*, LacChuB evolved laccase originally derived from *T. trogii*, and PO21B evolved VP originally derived from *P. eryngii* with CgL1SP,

CgR0949, and YwmC SPs, testing each of the nine possible Enzyme/SP combinations. Once the ligninolytic organism system was established and confirmed via Sanger Sequencing, assays were performed to assess lignin degradation effectiveness with the goal of detecting extracellular enzyme activity for at least one laccase and peroxidase expressing strain. Engineered *C. glutamicum* is hypothesized to be an effective platform for lignin depolymerization. Breaking down this hypothesis into sub-goals, it is hypothesized that: plasmids encoding lignin-modifying enzymes and the means for their secretion can be constructed and transformed into *C. glutamicum*; developed strains are viable and can secrete lignin-modifying enzymes; secreted enzymes can catalyze the oxidation of ABTS and the depolymerization of lignin; and lignin-degradation products from the engineered strain can be characterized and used for downstream applications. With the creation of a scalable, bacterial lignin degradation system, significant progress would be made toward waste valorization and a more sustainable world of production.

CHAPTER 2

METHODS

Strain development components

The plasmid *pCRB204* was used as a backbone to derive the nine constructs for the study. Preliminary cloning was performed in *E. coli* DH5-Alpha. *C. glutamicum* ATCC 13032 was utilized for final cloning and testing. Polymerase chain reaction (PCR) primers for cloning were obtained from Integrated DNA Technologies. All genes utilized in the study are summarized in **Table 2**.

Table 2: List of genes utilized. *Each gene in this study is included with short descriptions and sources.*

Label	Gene	Encoded Product	Acquirement
A	*cgl1*	CgL1, laccase endogenous to *C. glutamicum*[14].	PCR of *C. glutamicum* ATCC 13032 genomic DNA
B	*LacChuB*	LacChuB, laccase evolved by Mate et al. – codon-optimized for *C. glutamicum*. Originally from *T. trogii*[6].	Synthesis order from Twist Bioscience (attached to *cgl1SP*)
C	*PO21B*	PO21B, VP evolved by Garcia-Ruiz et al.– codon-optimized for *C. glutamicum*. Originally from *P. eryngii*[7].	Synthesis order from Twist Bioscience (attached to *cgR0949*)
1	*cgl1SP*	CgL1SP, TAT-pathway SP associated with CgL1 laccase endogenous to *C. glutamicum*[14].	Synthesis order from Twist Bioscience (attached to *LacChuB*)
2	*cgR0949*	CgR0949, High performance TAT-pathway SP endogenous to *C. glutamicum* R identified by Watanabe et al[21].	Synthesis order from Twist Bioscience (attached to *PO21B*)
3	*YwmC*	YwmC, high performance SEC-pathway SP endogenous to *Bacillus subtilis* identified by Brockmeier et al[23]. A *C. glutamicum* cleavage site was designed and added based on the study by Watanabe et al[21].	Incorporated as primer overhang for PCR with *PO21B*, ordered from Sigma Aldrich

Both heterologous enzyme genes (*LacChuB* and *PO21B*) were codon-optimized for *C. glutamicum*. A cleavage site was designed for YwmC SP based on the study by Watanabe et al. and was added to the 3' end of the sequence. The gene sequences endogenous to *C. glutamicum* were unaltered.

Each of the three enzyme genes were paired with each of the three SP genes for a total of nine combinations to test. **Figure 2** depicts the full factorial design of the

construct components and the corresponding naming scheme of the plasmids. Each enzyme gene has a BcuI and XhoI restriction site on either end, and each SP gene has a NotI and BcuI restriction site on either end enable Enzyme/SP gene attachment and attachment to the empty vector.

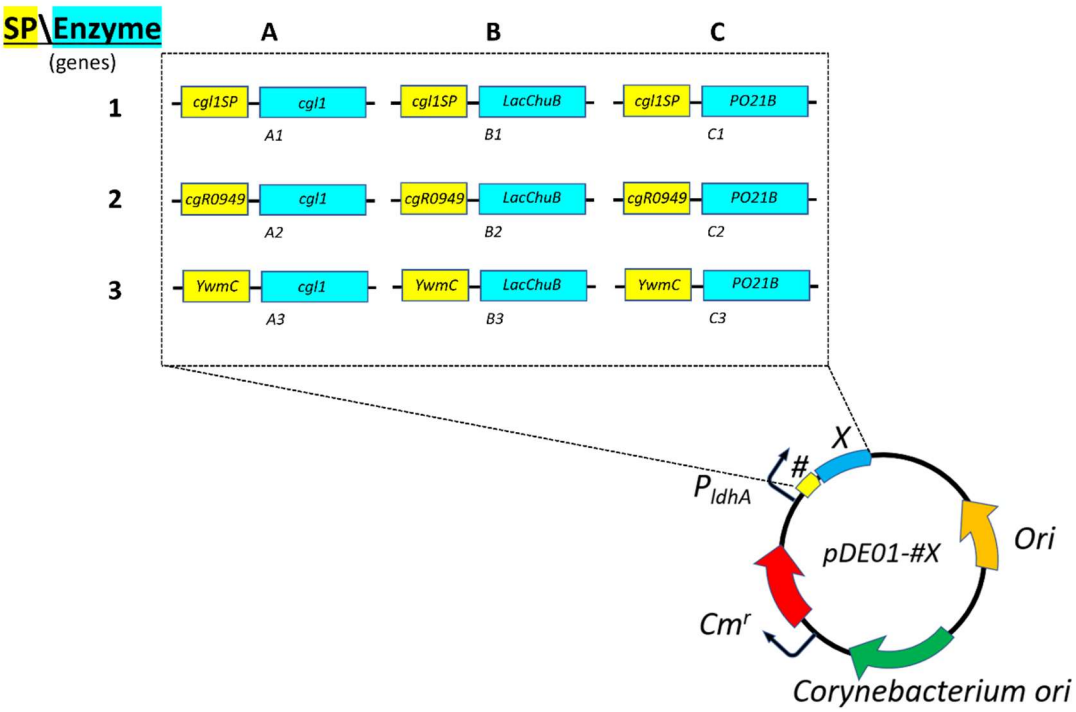

Figure 2: SP/Enzyme gene combination scheme. *Three enzymes were tested with three signal peptides each in a full factorial design, resulting in a total of nine constructs harboring the respective genes. The plasmid naming scheme is also conveyed by the figure. The pCRB204 backbone carries a Cm resistance gene, Cm^r, used for antibiotic marker selection.*

Each plasmid utilized in this study is listed in **Table 3**, and each primer utilized for cloning is listed in **Table 4.**

Table 3: List of plasmid constructs utilized.

Plasmid	Description	Source
pCRB204	*C. glutamicum* protein shuttle vector for production of D-lactic acid; carries Cm resistance	Okino et al.[18]
pDE01	*pCRB204* plasmid with *ldhA* gene removed and a MCS added with BsaI, NotI, EcoRV, BbsI, XhoI, SmaI, KasI, and AarI restriction sites.	*This study*
pDE01-A1	*pDE01* with *cgl1SP* - *cgl1* insert	*This study*
pDE01-A2	*pDE01* with *cgR0949* - *cgl1* insert	*This study*
pDE01-A3	*pDE01* with *YwmC* - *cgl1* insert	*This study*
pDE01-B1	*pDE01* with *cgl1SP* - *LacChuB* insert	*This study*
pDE01-B2	*pDE01* with *cgR0949* - *LacChuB* insert	*This study*
pDE01-B3	*pDE01* with *YwmC* - *LacChuB* insert	*This study*
pDE01-C1	*pDE01* with *cgL1SP* - *PO21B* insert	*This study*
pDE01-C2	*pDE01* with *cgR0949* - *PO21B* insert	*This study*
pDE01-C3	*pDE01* with *YwmC* - *PO21B* insert	*This study*

Table 4: List of primers utilized. *Restriction sites are bolded.*

Primer	Sequence	Purpose
BB-MCS-F	ATATA**CTCGAGCCCGGGGGCGCCCACCTGC** CTTCGACAACAACCTTGAATTGG	Cloning of *pDE01* from *pCRB204*
BB-MCS-R	ATATA**CTCGAGGAAGACGATATCGCGGCCG CGAGACC**TAATTGTCCCTCCGTTATTCCC	Cloning of *pDE01* from *pCRB204*
MCS-Verif-F	ACCACATTTTCGGACATAATCG	Sequencing and cPCR verification of all constructs
MCS Verif-R	AAAGGGATTTCTAAGCGGC	Sequencing and cPCR verification of all constructs
CgL1-F	ATATAA**CTAGT**GGTCCCTCCCTTCGCCC	Amplification of *cgl1* from *C. glutamicum genome*
CgL1-R	ATATA**CTCGAG**TTACTCGTAGCGAAGCGAG	Amplification of *cgl1* from *C. glutamicum genome*
A-Verif-F	TCGGCGATGTGATGTATCC	Sequencing verification of *cgl1*-containing constructs
A-Verif-R	ATACGTCCGTTGATGAGGTAG	Sequencing verification of *cgl1*-containing constructs
CgL1SP-F	ATATA**GCGGCCGC**ATGACAAGTAG	Amplification of *cgl1SP*
LacChuB-F	ATATAA**CTAGT**TCTATCGGCCCCGTG	Amplification of *LacChuB*
LacChuB-R	ATATA**CTCGAG**TTACTGATCGTCGGG	Amplification of *LacChuB*
B-Verif-F	TCAACCTGAAACCACAGACC	Sequencing verification of *LacChuB*-containing constructs
B-Verif-R	ATTGAGAACGAAGGAGTAGCG	Sequencing verification of *LacChuB*-containing constructs
CgR0949-F	ATATA**GCGGCCGC**ATGCAGATC	Amplification of *cgR0949*
PO21B-F	ATATAA**CTAGT**GCTACTTGTGATGATGGCAGG	Amplification of *PO21B*
PO21B-R	ATATA**CTCGAG**TTAAGAACGCGGCACG	Amplification of *PO21B*
C3-Ultra-F	TATA**GCGGCCGC**ATGAAGAAGCGCTTCTCCCT GATCATGATGACCGGCCTGCTGTTCGGCCTGA CCTCCCCAGCTTTCGCTGCACAGGAATCC**ACT AGT**GCTACTTGTGATGATGGCAGG	Addition of *YwmC* to *PO21B*
C-Verif-F	TTCCTGAGCCATTTGACTCG	Sequencing verification of *PO21B*-containing constructs
C-Verif-R	AACAACCACACCACTTCTGC	Sequencing verification of *PO21B*-containing constructs

Construction of multiple cloning site (MCS)

Before cloning the ligninolytic plasmids, an MCS had to be added to the *pCRB204* backbone to introduce restriction sites for the inserts and the *ldhA* gene had to be removed so the ligninolytic enzyme is the only protein expressed. *pCRB204* was amplified with primers excluding the *ldhA* gene. Both primers contained unique overhangs consisting of several restriction sites followed with XhoI at the 5' end. Once amplified, the linearized *pCRB204* no longer contained the *ldhA* gene, and each end of the amplicon contained a XhoI restriction site. A restriction digest (RD) was then performed on the amplicon using XhoI restriction enzyme (RE). The cut amplicon was then self-ligated to re-circularize the plasmid, forming *pDE01*. The process is illustrated in **Figure 3**.

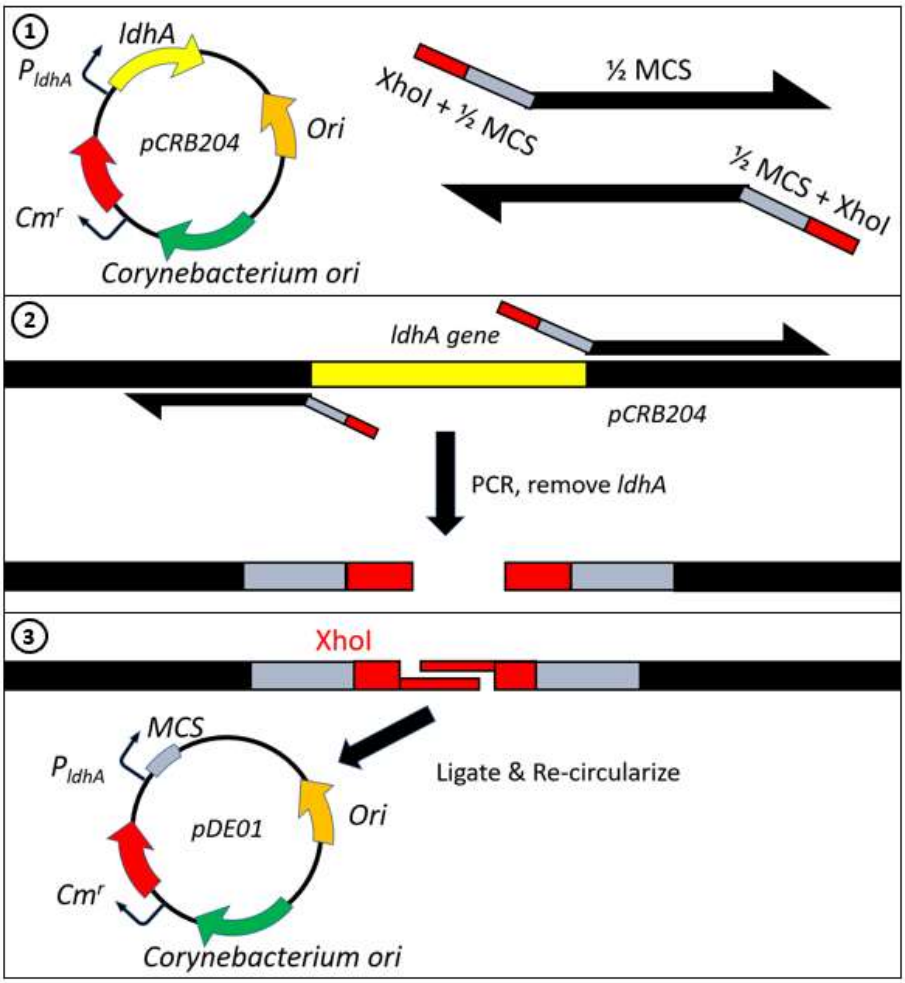

Figure 3*:* Construction of MCS. *From pCRB204, the pDE01 'empty' vector was cloned by excluding the ldhA gene in a full-plasmid PCR, adding half the MCS each as overhangs on each of the PCR primers, and performing restriction/ligation on the added XhoI site. The addition of the MCS allows for the cloning of the nine lignin-degrading plasmids via RD.*

Construction of lignin-modifying plasmids

With the new MCS of *pDE01* containing NotI and XhoI restriction sites, the lignin-degrading plasmids could be constructed via restriction cloning. The first two plasmids constructed were *pDE01-B1* and *pDE01-C2*, where the SP and enzyme genes were already attached as an insert from the original synthesis order. As in **Figure 4**, RD

with NotI and XhoI REs was performed on the insert and backbone. The cut sequences were gel purified and then ligated.

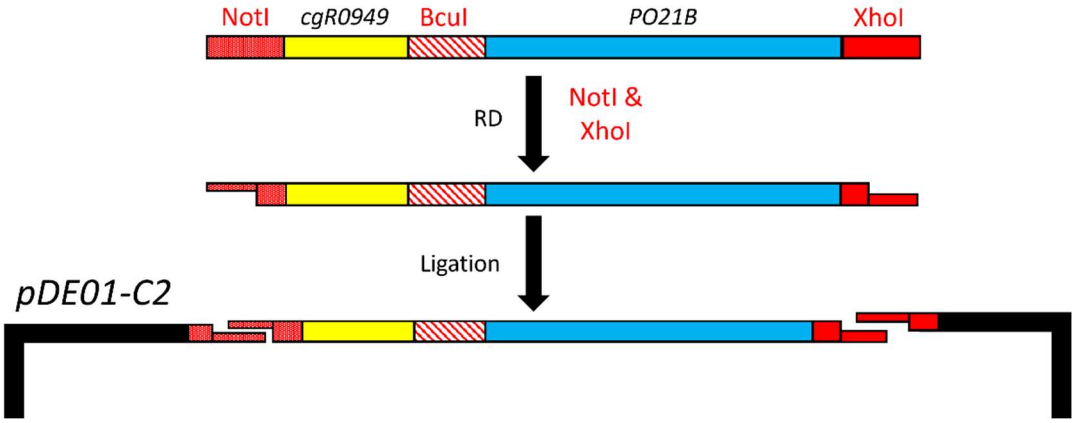

Figure 4: Cloning strategy for ordered SP/Enzyme gene combinations. *This first step cloned plasmids pDE01-B1 and pDE01-C2.*

Because the SP genes are small (<150 bp), they present potential problems if used alone as an insert. To incorporate *YwmC*, which was not pre-attached to an enzyme gene, an 'ultramer' was used. The SP gene was included to a long primer as an overhang and was attached to *PO21B* via PCR. This insert was cloned into the backbone via the same process as for the other pre-attached inserts to clone *pDE01-C3*. The primer design is depicted in **Figure 5**.

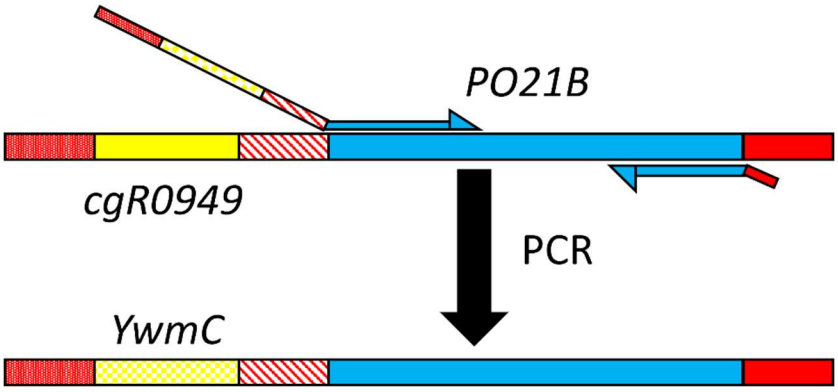

Figure 5: Cloning strategy for *YwmC* SP. *An ultramer containing YwmC as an overhang is utilized to combine YwmC and PO21B via PCR. Then, pDE01-C3 can be cloned with the same strategy depicted in* ***Figure 3****.*

Finally, the remaining six constructs were cloned via 'shuffling' of enzyme genes. RD was performed on the enzyme and backbone with BcuI and XhoI REs. The enzyme gene was cut out, but the SP gene remained attached to the backbone. The fragments were then gel purified and ligated. The 'enzyme shuffling' is shown in **Figure 6**.

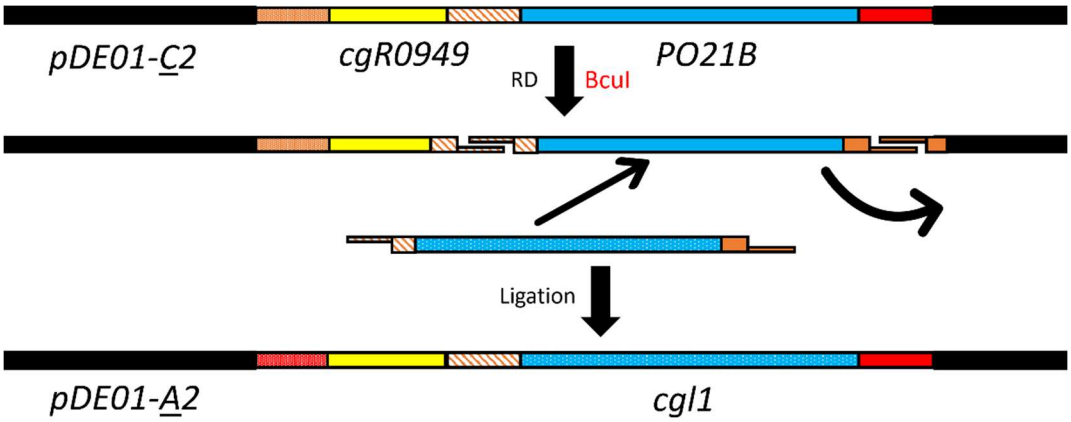

Figure 6: Cloning strategy for remaining constructs. *Using plasmids with established SP genes, enzyme genes were 'shuffled' via restriction digestion to clone the six other plasmids.*

Each plasmid constructed was transformed into *E. coli* DH5-Alpha competent cells via heat shock and plated onto Luria broth (LB)/Cm25 agar plates.

Plasmid verification

Plasmids were verified with three different techniques. For the first, colony PCR was performed on transformants to amplify the insert region. The length of the insert was compared to the expected length. If the colony PCR was successful, the transformant was grown in a seed culture, stored as a glycerol stock, and used for plasmid isolation. The second level of verification was by diagnostic RD. The isolated plasmid was cut with NotI, BcuI, and XhoI REs. The result was analyzed on a gel to confirm the correct lengths of vector, enzyme gene, and SP gene. Finally, the plasmids were confirmed via four Sanger Sequencing tests performed by GENEWIZ. The primer design for sequencing is depicted in **Figure 7**.

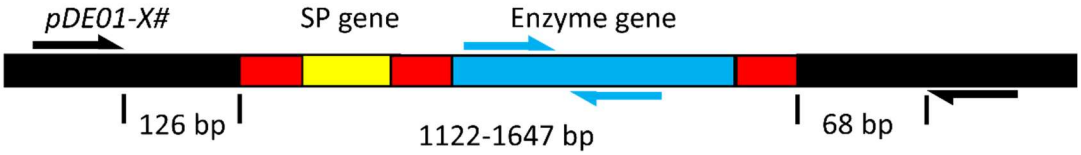

Figure 7: Sequencing primer design for verification of constructs.

Transformation into *C. glutamicum*

Prior to transformation to *C. glutamicum*, confirmed plasmids were transformed to and again harvested from *E. coli* GM272 to demethylate the plasmid DNA. The following procedure, modified from the work by van der Rest et al[24], was then followed to prepare competent cells and transform the constructed plasmids to *C. glutamicum*. First, wild type *C. glutamicum* ATCC 13032 was streaked onto brain-heart infusion (BHI) with sorbitol (BHIS) agar plates overnight. Then, two flasks of BHIS were inoculated and cultured overnight at 30 ºC and agitated between 225-250 rpm. The bacteria were then pelleted and resuspended in BHTG media (BHIS with Tween80 and

glycine) to make a 100 mL culture of optical density (OD) 0.3. This culture was again incubated until an OD of 0.9-1.0 was achieved. It was then sat on ice for 30 minutes. The bacteria were then pelleted again, and pre-chilled 10% glycerol solution was added. The cells then underwent four washes – pelleting the cells, decanting the supernatant, and resuspending again in 10% glycerol. Finally, the prepared competent cells were stored in a -80 ºC freezer.

For the transformation, the *C. glutamicum* competent cells were incubated on ice with an electroporation cuvette and the desired plasmid for about 20 min. Then, 0.5-1 uL (about 50-250 ng) of the plasmid was added and mixed with the competent cells. Once combined, the competent cells were loaded to the cuvette and incubated on ice for another 20 min. The cells were then electroporated at 2.5 kV, and 1 mL of BHI media was immediately added to resuspend the cells. The cells were then incubated at 46 ºC for 6 min before being incubated at 30 ºC for 2 hrs. Finally, the cells were plated onto BHI/Cm10 agar plates, and the acceptance of the plasmid verified via colony PCR following cell lysis. Herein, strains containing plasmids with genes encoding lignin-modifying enzymes (A1, A2, A3, B1, B2, B3, C1, C2, and C3) are referred to as 'experimental strains', and the strain containing the empty *pDE01* plasmid are referred to as the 'control strain'.

Growth assay of recombinant *C. glutamicum*

C. glutamicum viability and growth was tested in BTM2 defined media previously developed by Mhatre et al., containing in ultrapure water (per liter): 7 g $(NH_4)_2SO_4$, 0.5 g KH_2PO_4, 0.5 g K_2HPO_4, 0.5 g $MgSO_4 \cdot 7H_2O$, 11.1 mg $CaCl_2$, 0.2 mg biotin, 0.2 mg thiamine, 0.3 mg $FeSO_4 \cdot 7H_2O$, 0.5 mg $MnSO_4 \cdot H_2O$, 0.028 mg $ZnSO_4 \cdot 7H_2O$, 0.01 mg

$CuSO_4 \cdot 5H_2O$, 2 g urea, 8.4 g $NaHCO_3$, 2 mL 3-(*N*-morpholino)propanesulfonic acid (MOPS), and 20 g glucose, with 0.01 ug chloramphenicol added for antibiotic selection[25]. Duplicates of seed cultures for each strain were grown in 5 mL BHI overnight, and 50 uL of seed was inoculated to 5 mL BTM2 media to start growth testing. OD and thereby cell growth were monitored via measuring absorbance at 600 nm on a 96-well plate spectrophotometer. All growth occurred in culture tubes in a 30 ºC shaker running between 225-250 rpm.

Growth in expression media

To provide growth conditions geared toward increasing protein expression and favoring acidic pH for enzyme stability, BTM2 media was modified to create BTM2/BHI complex media. BTM2 has copper needed for laccase expression and iron and calcium chloride needed for VP expression, and undefined BHI promotes healthy cell growth. BTM2/BHI 18.5 g BHI powder per liter in addition to the components of BTM2, and 4% weight-per-volume (w/v) glucose instead of 2% (40 g instead of 20 g). Adjustments from naturally occurring pH 7 were made by the addition of citric acid.

To test growth in the new media and at different pHs, a seed culture of the control strain was grown in 5 mL BHI overnight, and 50 uL of seed was inoculated in duplicates to 5 mL BTM2/BHI media at pH 5, 6, and 7 to start growth testing. OD and thereby cell growth were monitored via measuring absorbance at 600 nm on a 96-well plate spectrophotometer. Expression cultures to be used for downstream *in vitro* testing were grown in various media for about 30 hours and collected by transferring 1 mL of culture to a centrifuge tube. Culture supernatant was separated from cell debris via centrifugation at max rpm for 5 min.

Drop assay for enzyme activity screening

To screen for enzyme activity, 2,2'-azino-bis(3-ethylbenzothiazoline-6-sulfonic acid) (ABTS) was used as a substrate. ABTS oxidation to its radical cation form ($ABTS^{\bullet+}$) is catalyzed by laccases and peroxidases, and also shows a color change from clear to dark blue-green. For the drop assay for quick screening, 10 uL of culture supernatant was added to 10 uL of ABTS buffer consisting of 3 mM ABTS and 0.1 mM H_2O_2 in 0.1 M tartrate buffer at pH 4. Enzyme activity in the supernatant is indicated by a color change to blue-green. For laccase positive controls, 1 uL of standard laccase from *Aspergillus* species in 9 uL of media was used in place of the supernatant, and for peroxidase positive controls, a pipette tip was touched to horseradish peroxidase and mixed into 10 uL of media.

ABTS plate assay for enzymatic activity

For quantification of enzyme activity, a more robust plate assay was performed with ABTS. The color change associated with the generation of $ABTS^{\bullet+}$ can be measured at a wavelength of 420 nm and is related to the concentration of $ABTS^{\bullet+}$ by the Beer-Lambert law, with the extinction coefficient (ε) of $ABTS^{\bullet+}$ being 36 $mM^{-1}cm^{-1}$. This change in $ABTS^{\bullet+}$ concentration is directly representative of enzymatic activity for the conversion of ABTS, with the unit 'U' being defined as the amount of enzyme required to convert 1 umol ABTS per minute. The Beer-Lambert law and sample calculations with error propagation are presented in **Appendix A**.

For the assay, 180 uL of ABTS buffer was added to wells of 20 uL of culture supernatants in a 96-well plate and briefly shaken. The absorbance at 420 nm was then measured in a kinetic cycle in a spectrophotometer at room temperature. For laccase

positive controls, 2.5 uL of standard laccase from *Aspergillus* species was mixed into 100 uL of the tested medium (BHI, culture supernatant, etc.) and 20 uL of the mixture used for the assay. For peroxidase positive controls, a pipette tip was touched to horseradish peroxidase and mixed into 500 uL of ultrapure water. Then 2 uL of this solution was mixed with 100 uL of the tested medium and 20 uL of the mixture used for the assay.

Statistical analysis

Independent, two-sided Student's t-tests were computed from summary statistics in R version 3.6.1 to assess significance in the differences in mean ABTS conversions across treatments.

CHAPTER 3

RESULTS

All plasmids have been constructed and sequenced

All plasmids were constructed and confirmed from DH5-Alpha via colony PCR, diagnostic RD, and Sanger Sequencing from GENEWIZ. An example of the sequencing verification results, viewed in Benchling, is shown in **Figure 8**.

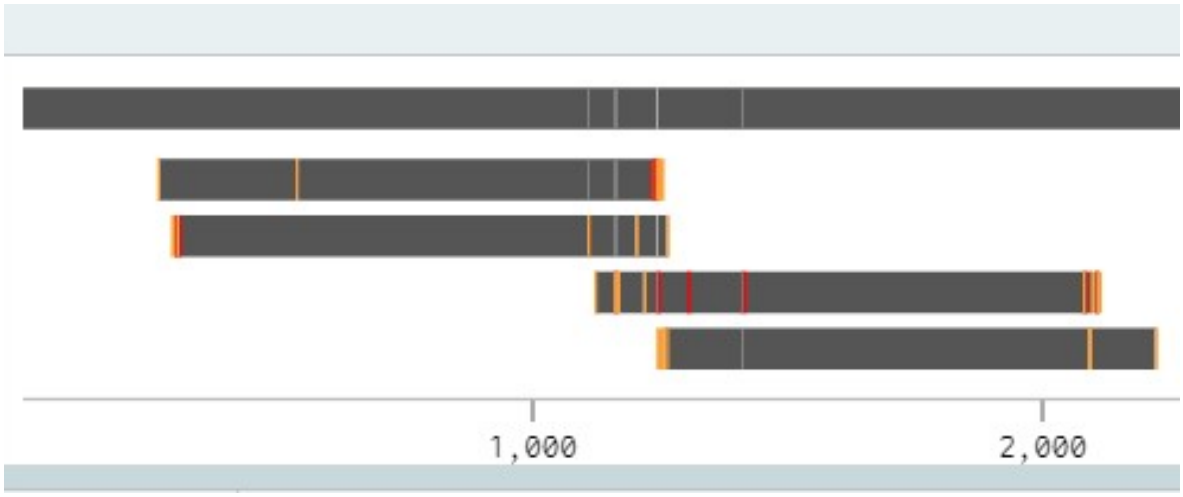

Figure 8: Pictorial sequencing results of *pDE01-B1*. *The plasmid identity was confirmed, despite lower accuracies at the ends of amplification.*

After analyzing the alignment, the 'marks' in **Figure 8** were determined to not be mutations but rather errors in amplification due to the amplification nearing its end. Sanger Sequencing was determined to be a necessary verification step, as one attempted construct showed a large deletion mutation in the SP gene. Although the deletion was not large enough to see on a gel, it caused a frameshift mutation which would have rendered the construct useless. **Figure 8** shows a confirmed sequencing result. Plasmids were then transformed into *E. coli* GM272, confirmed via colony PCR, and harvested to obtain the demethylated plasmids.

All engineered *C. glutamicum* strains have been developed and verified

Demethylated plasmids were then transformed into *C. glutamicum*, yielding transformants like those shown in **Figure 9**. Plasmid uptake was again verified via colony PCR, with example positive results viewed in gel electrophoresis being shown in **Figure 10**.

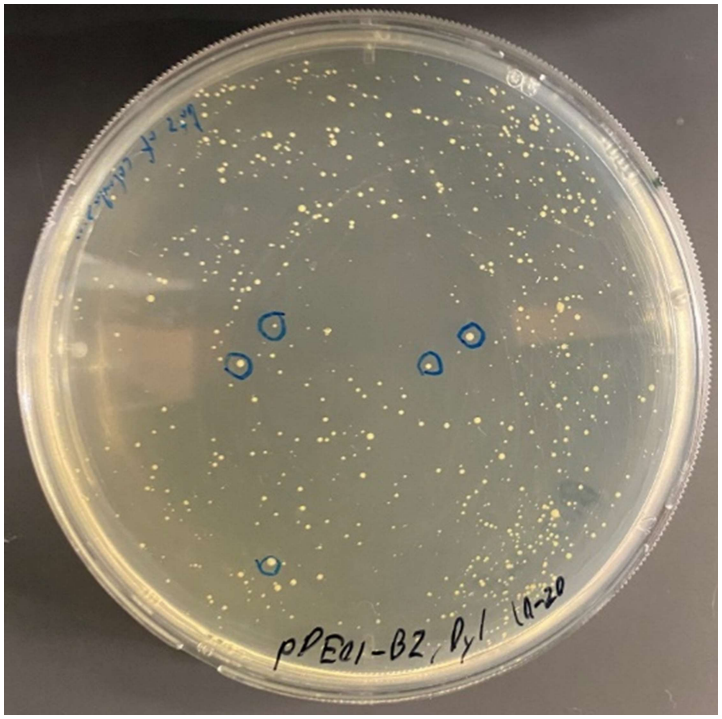

Figure 9: Plate of *C. glutamicum* transformants. *Electroporation showed high transformation efficiency, yielding many colonies with positive colony PCR results.*

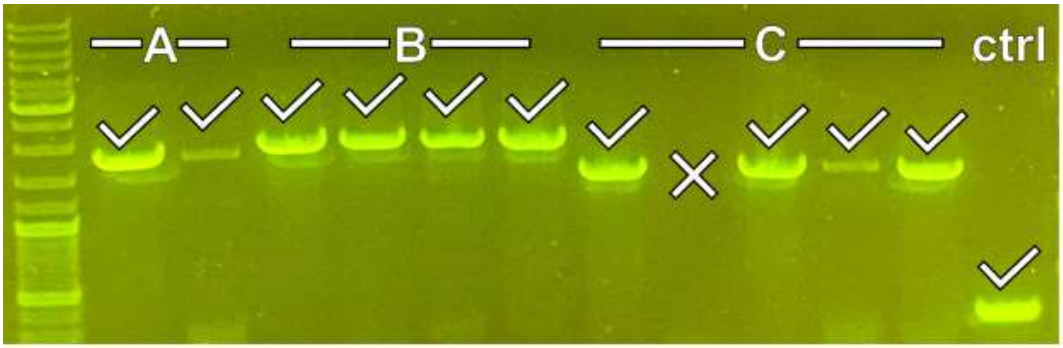

Figure 10: Sample gel electrophoresis from colony PCR confirming plasmids in *C. glutamicum* transformants. *Bands obtained from colony PCR show the expected length of DNA.*

All constructed strains of *C. glutamicum* yielded positive results when verifying the plasmid content.

Growth curves of all recombinant strains were not substantially altered

All confirmed experimental strains grew in BTM2 media at a rate comparable to the control strain. Most strains grew slightly slower than the control, with the 'B2' strain being the slowest. The 'B3' and 'C2' strains were the fastest and grew slightly faster than the control strain. In general, strains transitioned from lag to log phase at around six hours, and from log to stationary at around 24 hours. The time for entering the death phase was inconsistent across strains with some ('A1', 'A3', 'C1', 'C2') decreasing in cell density between 30-40 hours and some ('B1', 'B2', 'B3') not decreasing until 48 hours were reached. Strains also achieved similar maximum cell densities, however strains 'A3' and 'C3' were noticeably less dense than the control strain at 48 hours. Growth curves for each experimental strain are described and compared to the control strain in **Figure 11**.

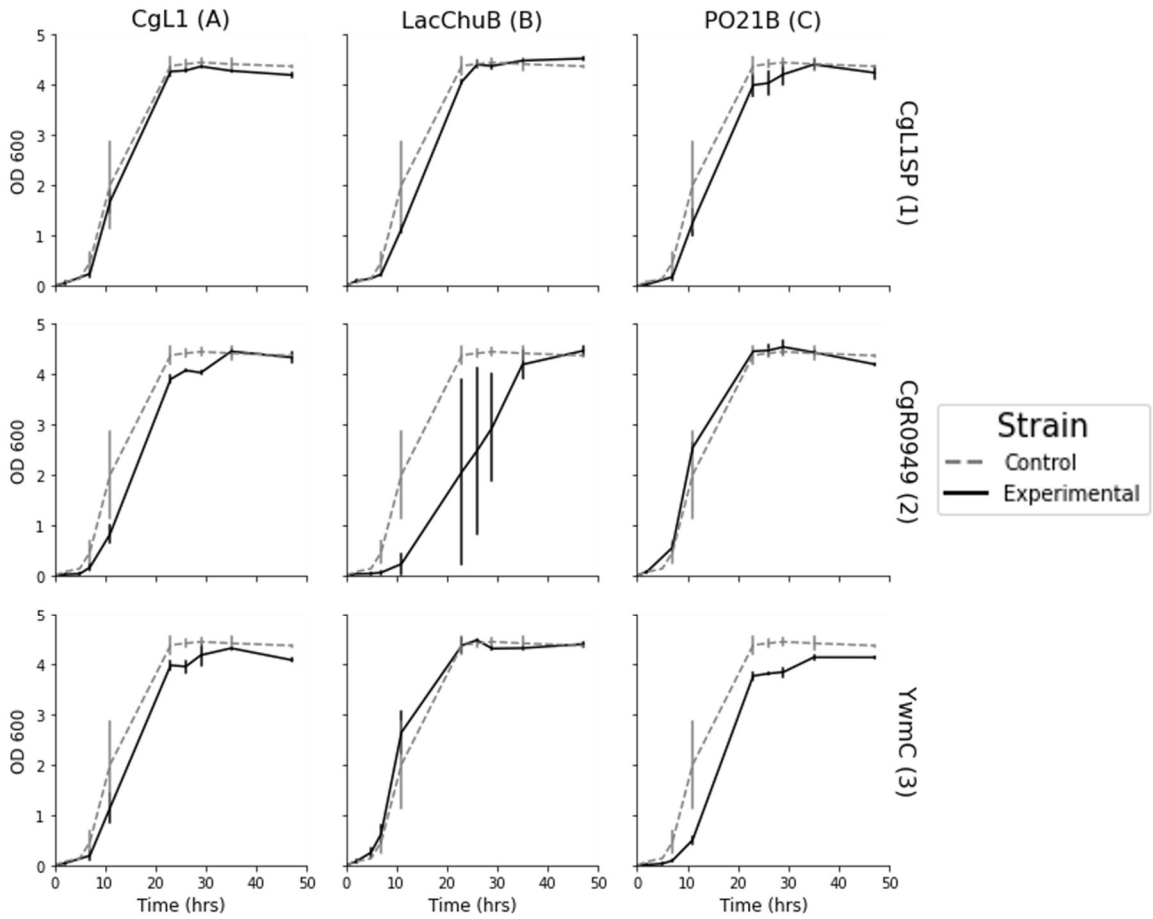

Figure 11: Growth curves of recombinant *C. glutamicum* strains in BTM2 media. *Each experimental strain is plotted with the control strain for comparison. Error bars represent the 95% confidence interval of measurements from duplicates.*

Growth in expression media occurs at a range of pHs

The control strain was able to grow in the new BTM2/BHI media at pH 5, 6, and 7. At pH 6 and 7, cells entered the log phase around 8 hours and the stationary phase around 24 hours, similar to growth in BTM2 media. The stationary-phase cell density of cells grown in BTM2/BHI at pH 7 were comparable cells grown in BTM2 (OD about 4.3), but the cells grown at pH 6 had lower cell density. Cells grown at pH 5 grew slower, entering log phase at around 12 hours and stationary phase at around 30 hours, and had

slightly lower stationary-phase cell density than those grown at pH 6. Growth curves of the control strain in BTM2/BHI at different pHs are shown in **Figure 12**.

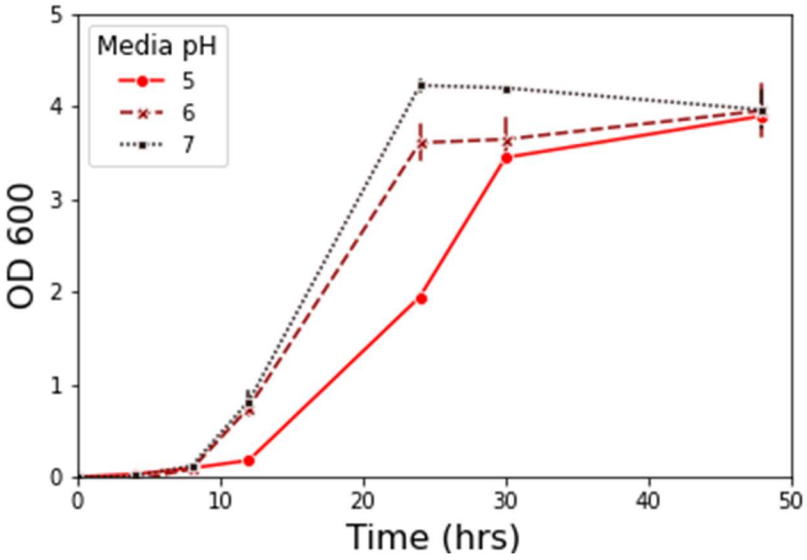

Figure 12: Growth curves of control strain at different pHs of BTM2/BHI media. *Error bars represent the 95% confidence interval of measurements from duplicates.*

Recombinant strains exhibit undetectable ABTS activity

At present, ABTS assays have not detected lignin-modifying enzyme activity in developed *C. glutamicum* strains. **Figure 13** shows the results of one drop assay of all peroxidase strains ('C1', 'C2', 'C3') grown in BTM2/BHI at pH 5, 6, and 7, where none exhibited the expected color change. Similarly, the plate assay tests on experimental strains did not show the anticipated increase in absorbance associated with $ABTS^{\bullet+}$ over time. Multiple minor adjustments were made in the experimentation for the assays including lysing the cells to test for intracellular enzyme expression as opposed to only expression in the supernatant; supplementing the cultures and supernatants with up to 2 mM $CuSO_4 \bullet 5H_2O$, 2 mM $FeSO_4 \bullet 7H_2O$, and 1 mM $CaCl_2$ for laccase and peroxidase

expression; adding extra H_2O_2 in drop assays; and testing different media; and incubating the reactions for longer time at greater temperatures. These variations also did not yield positive results. Photographic results of these drop assay variations are presented and discussed in **Appendix B**.

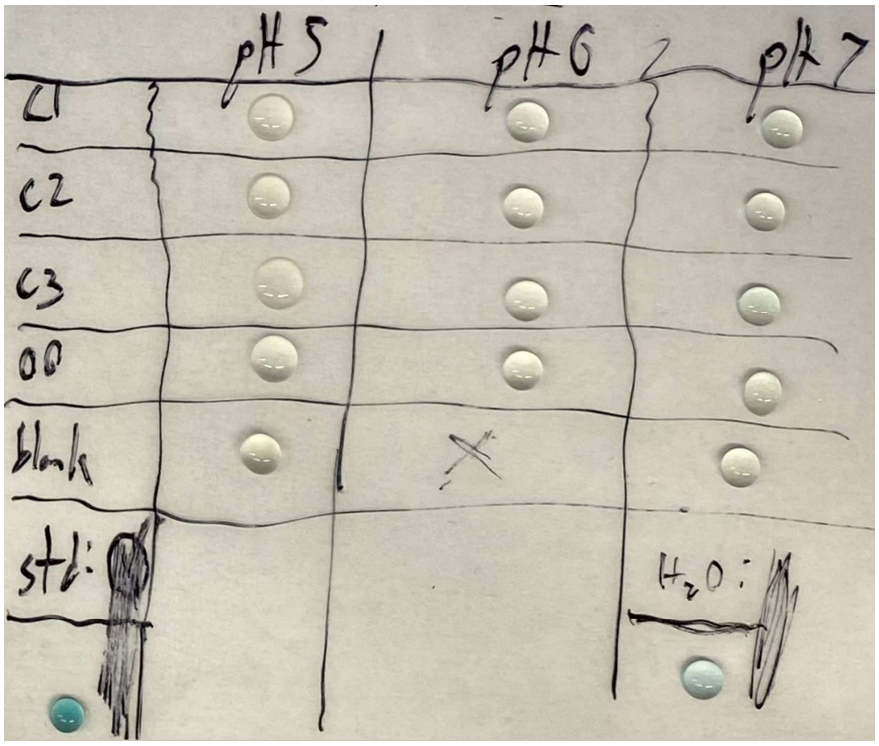

Figure 13: Photographic results of peroxidase strain drop assay. *Cells were grown in BTM2/BHI media at multiple pHs. 'OO' represents the control strain. No culture supernatant exhibited the blue-green color change associated with enzymatic activity on ABTS seen in the positive control standard shown ('std').*

Positive control ABTS activity is decreased in culture medium

A purchased laccase and horseradish peroxidase were tested in the ABTS assays as positive controls. For the laccase drop assay, notably less enzyme activity was seen in BHI media relative to water. Several minutes were needed for the reaction to progress to completion. Photographic results of the laccase assays are given in **Figure 14**.

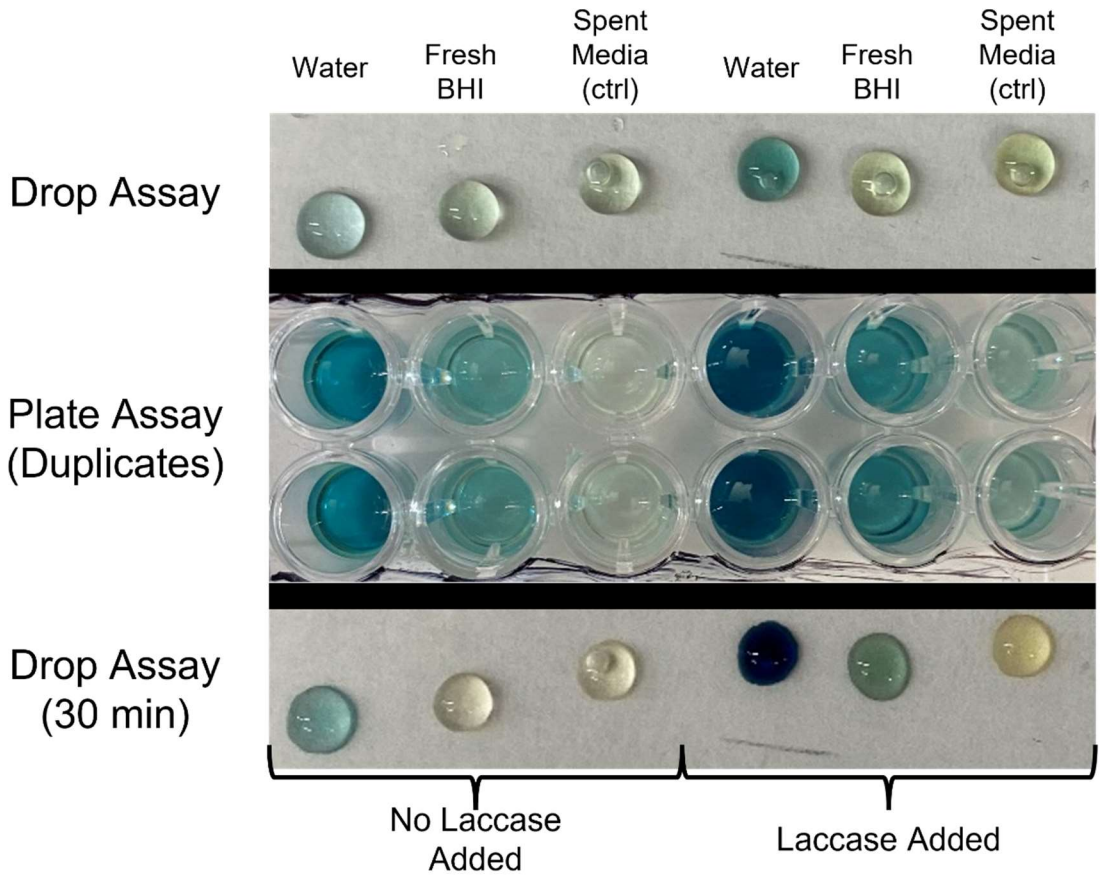

Figure 14: Photographic results of laccase positive control assays. *The beginning of the drop assay is shown at top, a picture of the plate assay is shown in the middle, and the drop assay after 30 minutes is shown at bottom. Reactions in water, fresh BHI media, and control strain supernatant (BHI media) were tested. The left three columns of reactions are with no added laccase, and the right three have laccase added, as seen by the darker blue-green coloration. Reactions in media are visibly lighter than reactions in water. Bubbles in the drop assay were due to pipetting.*

Laccase positive control plate assay data over time are shown in **Figure 15** and overall results are summarized in **Figure 16**. Change in absorbance for each reaction followed a consistent linear trend. The laccase was concentrated enough that enzyme activity produced an absorbance of greater than 4, which is above the maximum readable by the spectrophotometer. The laccase reaction in water occurred much more rapidly than those in BHI media, and the reactions did not occur when no laccase was added. Despite

the same amount of laccase being added to all three reactions, the perceived enzymatic activity in water was about 10.91 U/L, whereas in fresh BHI and control strain supernatant it was about 7.56 and 7.42 U/L, respectively. These measures considered the slight change in absorbance occurring in media with no added laccase, with a decrease in absorbance of only about 0.018 occurring in the reaction in water with no added laccase, but a decrease of about 0.15 and 0.18 occurring in reactions in fresh BHI and control strain supernatant, respectively. The enzymatic activities in media were significantly lower than in water ($p < 0.01$, Student's t-test).

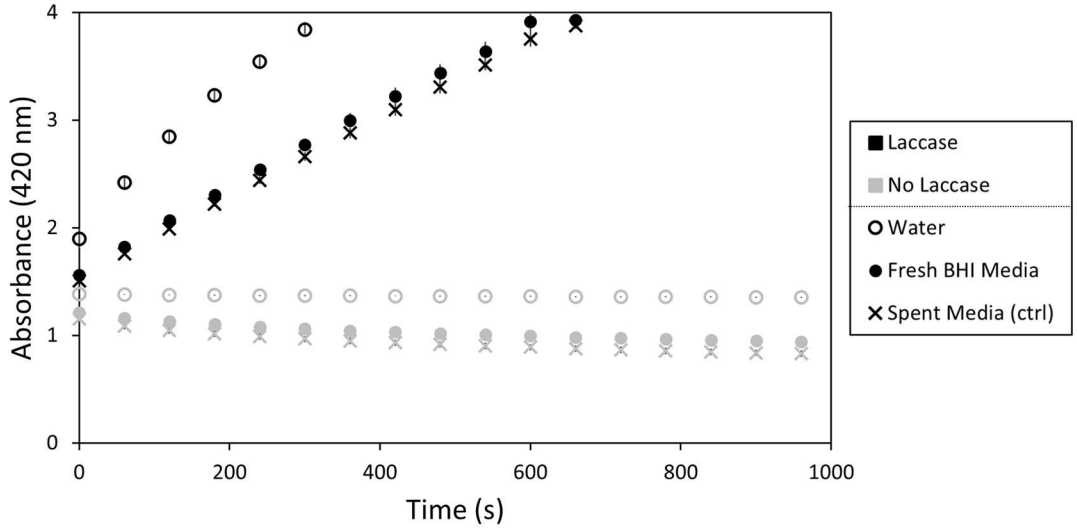

Figure 15: Time plot of absorbance readings from laccase positive control plate assay. *Error bars represent the sample standard deviation from duplicate measures. Absorbance readings over 4 throw an error on the spectrophotometer.*

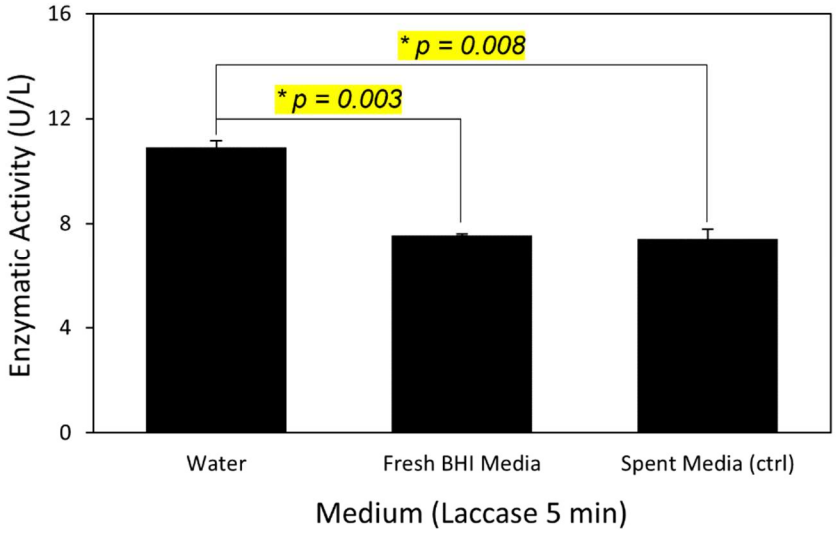

Figure 16: Bar plots of enzymatic activity for laccase positive control plate assay. *Error bars represent the sample standard deviation from duplicate measures; p-values were determined by independent, two-sided Student's t-test.*

For the peroxidase drop assay, notably less enzyme activity was seen in BHI media relative to water, and even less so in control strain supernatant relative to fresh BHI media or peroxidase strain ('C3') supernatant. Results were visualized quicker than laccase drop assay results. After several minutes, blue-green coloration of reaction faded. Addition of extra H_2O_2 for better visualization of peroxidase expression (1 uL, 30%) also caused culture supernatant, but not water or fresh media, to effervesce. Photographic results of the peroxidase assays are given in **Figure 17**.

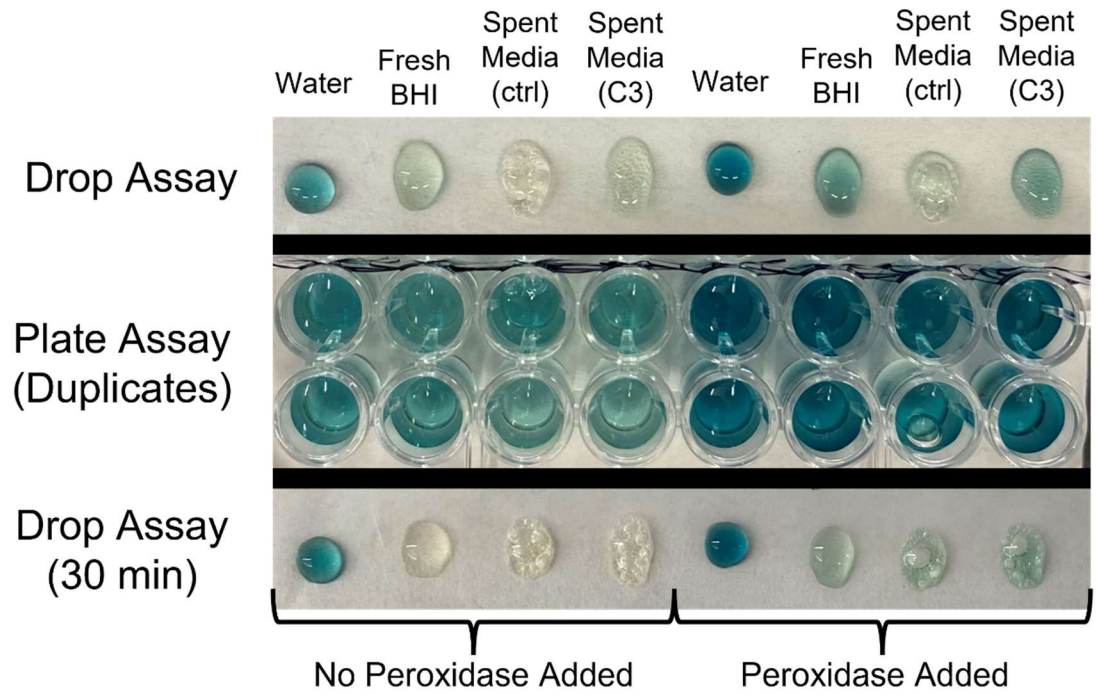

Figure 17: Photographic results of peroxidase positive control assays. *The beginning of the drop assay is shown at top, a picture of the plate assay is shown in the middle, and the drop assay after 30 minutes is shown at bottom. For the drop assays, 1 uL of 30% H_2O_2 was added to each reaction for better visualization. Reactions in water, fresh BHI media, control strain supernatant (BHI media), and a peroxidase strain supernatant ('C3', BHI media) were tested. The left four columns of reactions are with no added laccase, and the right three have laccase added, as seen by the darker blue-green coloration. Reactions in media are visibly lighter than reactions in water, and even lighter in spent media. Bubbles visibly effervesced in supernatant reactions.*

Peroxidase positive control plate assay data over time are shown in **Figure 18** and overall results of enzymatic activity are summarized in **Figures 19 & 20**. At lower time points, the change in absorbance followed a mostly linear trend, but eventually tapered off at a maximum. Initial changes in absorbance were similar across different medias, with the reaction in peroxidase strain ('C3') strain supernatant being the quickest by a small margin. However, the reaction in 'C3' supernatant achieved a maximum notably lower than reactions in water and fresh BHI media. Reactions did not appear to occur in

any of the medias when no peroxidase was added, but the reactions in water showed a slight increase in absorbance over time.

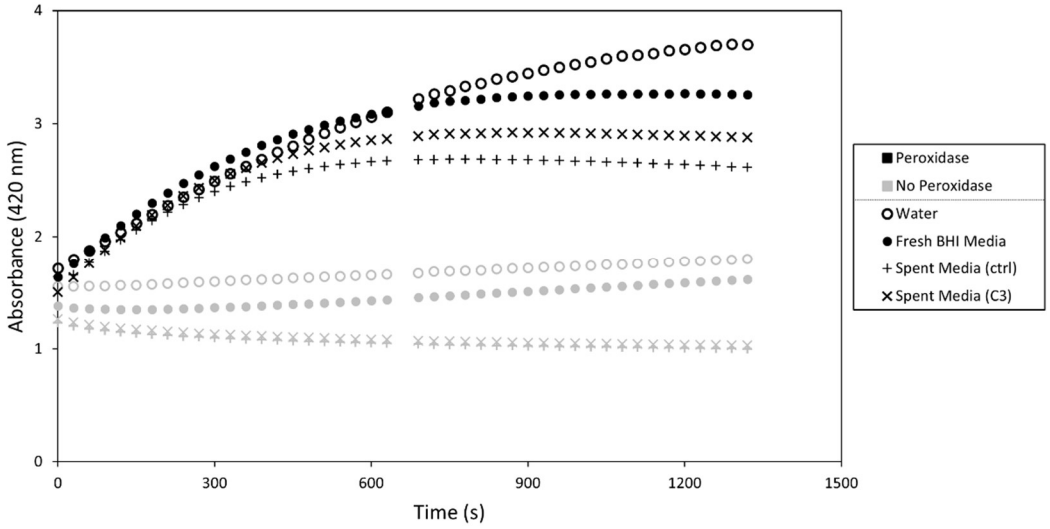

Figure 18: Time plot of absorbance readings from one replicate of the peroxidase positive control plate assay. *Figures for the other replicate and the average are included in **Appendix C**.*

The perceived enzymatic activities of reactions in each media were different depending on which time points were chosen for analysis. **Figure 19** shows a summary of calculated enzymatic activity at 5 minutes, while **Figure 20** reports enzymatic activity based on measurements after 20 minutes. At 5 minutes, reactions in C3 culture supernatant appeared to have the greatest enzymatic activity (about 5.77 U/L) whereas reactions in water appeared to have the least (about 4.14 U/L). At 20 minutes, however, reactions in water appear to have the highest enzymatic activity (about 2.38 U/L) whereas reactions in C3 and control strain supernatant appear to have the lowest (about 1.75 and 1.51 U/L, respectively). These differences at both time points were not statistically significant. When not correcting for the change in absorbance of the media without added

horseradish peroxidase, the changes in absorbance in each media are similar after 5 minutes, but after 20 minutes the change in absorbance is significantly greater in water than in control strain supernatant and approaches significance for being greater than in C3 supernatant ($p = 0.101$). Results of unadjusted changes in absorbance are provided in **Appendix D**.

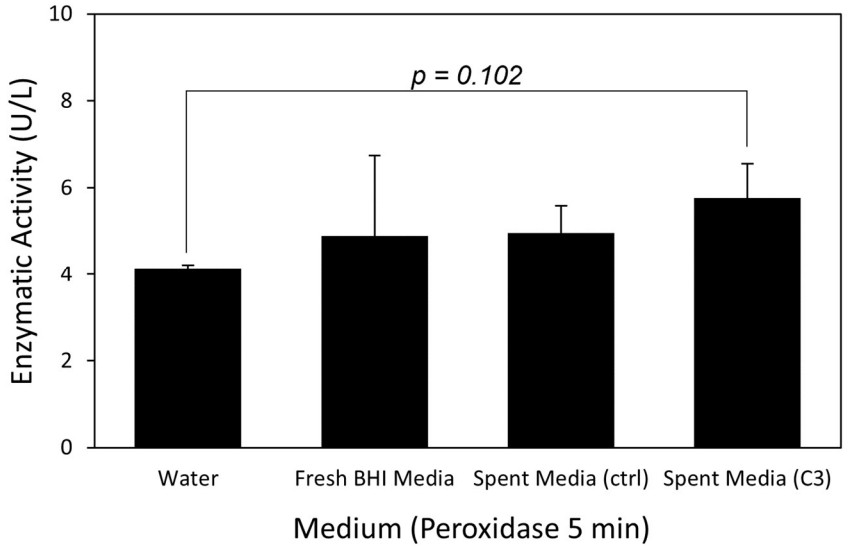

Figure 19: Bar plots of enzymatic activity for positive control peroxidase plate assay after 5 minutes. *Error bars represent the sample standard deviation from duplicate measures; p-values were determined by independent, two-sided Student's t-test.*

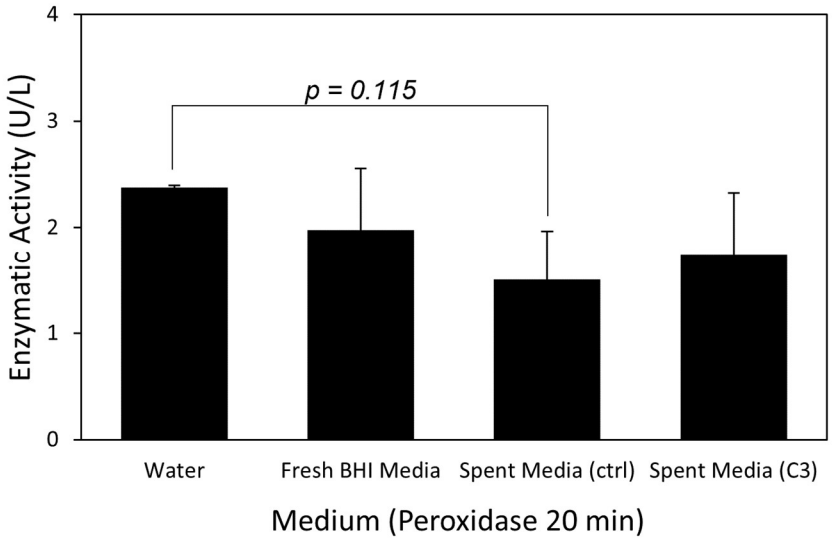

Figure 20: Bar plots of enzymatic activity for positive control peroxidase plate assay after 20 minutes. *Error bars represent the sample standard deviation from duplicate measures; p-values were determined by independent, two-sided Student's t-test.*

Across both laccase and peroxidase testing, enzymatic activity generally was decreased in BHI media relative to water. At early time points, perceived peroxidase activity was perceived to be greater in experimental strain supernatant, but there was high variability in measurements. Laccase activity was significantly greater in water than in culture supernatant. Supernatants effervesced when supplied with H_2O_2.

CHAPTER 4

DISCUSSION

Recombinant ligninolytic *C. glutamicum* is viable

From the positive sequencing results and strong growth curves, *C. glutamicum* can be engineered to host lignin-modifying genes and has potential as a platform for lignin depolymerization. All engineered strains were able to be constructed, were validated by sequencing, and retained the plasmid after prolonged growth (judged by a repeated PCR). Furthermore, all engineered strains grew at similar pace to the control strain, suggesting the metabolic cost of expressing the recombinant genes is not detrimental, nor are the products cytotoxic.

The lack of hindrance in strain growth in a range of pHs and media also lends support to use of *C. glutamicum* for lignin depolymerization. Many of the high-performing lignin-modifying enzymes display optimal performance at acidic pHs, like the evolved fungal enzymes tested in this study. Because *C. glutamicum* cultures are both viable at acidic pHs up to 5 and known to grow well in alkaline environments up to pH 9, *C. glutamicum* could be a great platform for developing bio-based processes using these enzymes. The wide range of available pHs to test would be helpful as process conditions for lignin depolymerization and subsequent assimilation are tested and optimized.

There exists a barrier to current strains' enzyme expression

Despite retention of the constitutively expressed plasmid, enzyme activity was not detected in the supernatant of the constructed strains. There exist several areas of opportunity for disruption of lignin-modifying enzyme expression throughout the process. Furthest upstream, it is possible the genes encoding the SP/lignin-modifying

enzyme combo is not being expressed. This is thought to be unlikely because the *pCRB204* backbone used is well established and has been used successfully for other projects in the same lab. Transcription and translation efficiency may be decreased by the lack of a terminator sequence downstream of the lignin-modifying enzyme gene, but this should not hinder enzyme expression at the level seen.

Another area with opportunities for disruption of enzyme expression is post-translational protein modification/folding and secretion. Protein misfolding is one primary concern in this area. The lack of eukaryotic chaperone proteins and other post-translational modification capabilities in *C. glutamicum* may impair heterologous fungal enzyme folding, but this would not be a problem for the native CgL1 laccase in 'A' strains. SP sequence structures may disrupt folding of the enzyme as well. It is also worth considering that the BcuI restriction site between the SP and enzyme gene would be translated to threonine-serine and would likely not be cleaved by the SPase. These extra two amino acids could thus have an influence on protein folding before and after SP cleavage, potentially impairing both enzyme secretion and activity. If the lack of enzyme expression in the supernatant is only due to problems with secretion it would be expected to see positive ABTS results when using cell lysates, however this test also yielded negative results (**Appendix B, Figure B-3**).

The furthest possible 'downstream' problem is that the enzyme is correctly folded and secreted but for some other reason is unable to act upon the ABTS substrate. Several possible reasons for this exist. One is the possibility of a chemical agent reversibly inhibiting the enzyme, for example through either competing with ABTS to bind the enzyme as a substrate or 'blocking' the enzyme-ABTS complex from releasing

converting and releasing $ABTS^{\bullet+}$ product. For laccases, enzyme activity decrease could also occur due to copper binding sites being empty or occupied by an inhibitor. Another is the irreversible inhibition of the enzyme or the degradation of either the enzyme or ABTS. One reason for selecting *C. glutamicum* was its low extracellular protease activity, however the possibility for enzyme degradation by the strain remains. Finally, another potential cause is the decrease of availability of oxidizing agent (O_2 for laccase and H_2O_2 for peroxidase). Positive control assays performed in this study provide insight into these possibilities.

Enzyme activity may be disrupted by culture medium and metabolism

For the laccase positive control tests, enzyme activity was significantly decreased in both fresh and spent media relative to water despite using the same amount of enzyme, suggesting BHI media components may be inhibiting the laccase. Several compounds are capable of inhibiting laccases. One study showed that mercaptopurine, thioguanine, captopril, dimercaptopropanol, and dimercaptosuccinate competitively inhibited laccase[26]. Another study focusing on copper-chelating agents showed that ethylenediaminetetraacetic acid (EDTA), citric acid, oxalic acid, malonic acid, sulphamic acid, and hydroxylammonium chloride all inhibited laccase[27]. The same study showed laccase activity to be enhanced by Cu^{2+} up to 1 mM but inhibited by Cu^{2+} at higher concentrations, and to be strongly inhibited by cadmium[27]. Cl^- and OH^- are also able to inhibit laccase[28]. BTM2 media used in this study contained 0.04 uM Cu^{2+} added as $CuSO_4 \bullet 5H_2O$ and 0.2 mM Cl^- added as $CaCl_2$. Additional Cu^{2+} was added after cell growth to a concentration of 0.4 mM and 2 mM in one test to ensure Cu^{2+} was available for copper binding sites in laccase, but still did not yield detectable enzyme activity in a

drop assay (**Figure B-4**). Finally, laccase is competitively inhibited by compounds produced from the depolymerization of lignin[29]. While less relevant for troubleshooting current inhibitory effects, this is an important consideration for future experiments and for the development of a robust lignin depolymerization process using laccase. From a different perspective, it could also be possible that O_2 is less available in BHI media relative to water, which would decrease laccase activity, but these potential mechanisms are unknown.

For the peroxidase positive control tests, calculated differences in enzyme activity across reaction media were not statistically significant, but the unadjusted change in absorbance associated with $ABTS^{\bullet+}$ after 20 minutes was significantly lower in control strain supernatant than in water (**Figure D-3**). Drop assay results also showed visibly less blue-green coloration in reactions in media relative to water, with reactions in culture supernatant having less color change than those in fresh media. These results suggest that BHI components and/or cellular metabolism products may be inhibiting peroxidase activity. Bovine serum albumin is one agent that has been previously shown to competitively inhibit horseradish peroxidase[30]. Inhibition by bovine serum albumin is important to note because similar protein might be present in BHI media. NADH is another important molecule shown to competitively inhibit peroxidase[31]. NADH is noteworthy because it is a crucial compound in the electron transport chain in *C. glutamicum* nearly all bacteria and mitochondria in eukaryotes[32,33]. Cadmium is also a strong, irreversible inhibitor of horseradish peroxidase[34]. Humic acid and fulvic acid have also been shown to inhibit horseradish peroxidase anti-competitively, and luteolin has been shown to inhibit horseradish peroxidase non-competitively[30,35].

Effervescence of culture supernatants, but not water nor fresh BHI media, when supplied with H_2O_2 also suggests compounds produced by *C. glutamicum* are reacting with and decreasing the availability of H_2O_2, which would result in lower peroxidase activity. Pyruvate could be one molecule responsible. Pyruvate is a central molecule to glycolysis and the citric acid cycle, but is also a strong scavenger of H_2O_2[36,37]. The reaction between pyruvate and H_2O_2 produces acetate, water, and CO_2[36,37]. The produced CO_2 could explain the observed effervescence. Pyruvate is a component of some cell culture media and protects cells against the cytotoxic effects of oxidants like H_2O_2[36,37]. However, because the effervescence was not observed in fresh media, pyruvate reacting with H_2O_2 in this study are likely from the metabolism of *C. glutamicum* rather than from the BHI media.

For both laccase and peroxidase positive control tests, BHI media components seemed to inhibit enzyme expression, with significantly lower enzyme activity or change in absorbance in media relative to water even with incredibly low statistical power of only two replicates. Completing more tests and replicates would be desirable not only to confirm these results but to also reduce variance in measures, provide more statistical power to judge significance in differences in enzyme expression between medias, and detect outliers.

Future experimentation

Many tests could be completed to further diagnose the lack of enzyme expression in the constructed strains. To verify transcription of the lignin-modifying enzyme genes is occurring, real-time quantitative PCR could be performed. To verify any amount of desired enzyme is produced and secreted, protein purification and characterization

techniques such as SDS-PAGE (sodium dodecyl sulfate-polyacrylamide gel electrophoresis) could be used. A Bradford assay could be used to quantify the total amount of protein produced or secreted by the experimental strains as another method to measure and determine whether enzymes are being expressed and secreted. Substrates other than ABTS could be used for testing enzymatic activity, such as 2,6-dimethoxyphenol (DMP), guaiacol, or syringaldazine. Because ABTS has lower substrate affinity for laccase than DMP and syringaldazine, these other substrates may provide better or more accurate results[27]. To address the potential issues with enzyme inhibition, expression media must be developed and optimized for lignin-modifying enzyme expression by *C. glutamicum*. A method must also be devised to avoid enzyme expression disruption or the depletion of H_2O_2 by *C. glutamicum* metabolism products such as pyruvate.

Once the source of enzyme activity disruption is identified and remedied, experimental strains exhibiting strong performance in ABTS assays would be tested in fermentations with lignin as a substrate. Strains will be grown in optimized expression medias containing alkaline lignin, dealkaline lignin, and sodium lignosulfonate. Culture supernatants will then be sampled and tested to characterize lignin degradation products via gas chromatography-mass spectrometry and nuclear magnetic resonance. From these results, the strain's ability to depolymerize specific bonds of lignin will be assessed and lignin-derived products will be identified, providing insight to downstream assimilation opportunities. Later testing would be performed for developing coculture or sequential culture processes, eventually leading to and providing insight for the development of bioreactors and biorefineries for waste valorization to scale.

CHAPTER 5

CONCLUSION

In this study, nine strains of *C. glutamicum* containing plasmids encoding lignin-modifying enzymes and SPs for their secretion were constructed. Positive sequencing results and growth comparable to a control strain in a range of pHs support the hypothesis that *C. glutamicum* is a strong candidate for developing a lignin depolymerization platform. At the current stage in testing, however, enzyme activity of constructed strains has not been detected. Testing the activity of known purified lignin-modifying enzymes at the same conditions revealed a decrease in enzyme activity in culture media and culture supernatants relative to water. Effervescence of culture supernatant but not water nor fresh culture media when subject to H_2O_2 also suggests cellular metabolism byproducts are reacting with H_2O_2, reducing its availability for peroxidase reactions. Because of these results, it is now hypothesized that culture media components or cellular metabolism byproducts are disrupting enzyme expression via enzymatic inhibition and the decrease of necessary oxidizing agents (O_2 and H_2O_2). These findings are informative for future troubleshooting and for other research to optimize media for specific enzyme expression. More investigation is needed to verify the efficacy of a *C. glutamicum* platform for lignin depolymerization, but this work creates headway toward the goal of sustainable waste valorization.

REFERENCES

1. Pollegioni L, Tonin F, Rosini E. Lignin-degrading enzymes. *FEBS J*. 2015;282(7):1190-1213. doi:10.1111/febs.13224

2. Becker J, Wittmann C. A field of dreams: Lignin valorization into chemicals, materials, fuels, and health-care products. *Biotechnol Adv*. 2019;37(6):107360. doi:10.1016/j.biotechadv.2019.02.016

3. Lee S, Kang M, Bae JH, Sohn JH, Sung BH. Bacterial Valorization of Lignin: Strains, Enzymes, Conversion Pathways, Biosensors, and Perspectives. *Front Bioeng Biotechnol*. 2019;7:209. doi:10.3389/fbioe.2019.00209

4. Santhanam N, Vivanco JM, Decker SR, Reardon KF. Expression of industrially relevant laccases: prokaryotic style. *Trends Biotechnol*. 2011;29(10):480-489. doi:10.1016/j.tibtech.2011.04.005

5. Gonzalez-Perez D, Alcalde M. Assembly of evolved ligninolytic genes in *Saccharomyces cerevisiae*. *Bioengineered*. 2014;5(4):254-263. doi:10.4161/bioe.29167

6. Mate DM, Gonzalez-Perez D, Falk M, et al. Blood Tolerant Laccase by Directed Evolution. *Chem Biol*. 2013;20(2):223-231. doi:10.1016/j.chembiol.2013.01.001

7. Garcia-Ruiz E, Gonzalez-Perez D, Ruiz-Dueñas FJ, Martínez AT, Alcalde M. Directed evolution of a temperature-, peroxide- and alkaline pH-tolerant versatile peroxidase. *Biochem J*. 2012;441(1):487-498. doi:10.1042/BJ20111199

8. Maté D, García-Burgos C, García-Ruiz E, Ballesteros AO, Camarero S, Alcalde M. Laboratory Evolution of High-Redox Potential Laccases. *Chem Biol*. 2010;17(9):1030-1041. doi:10.1016/j.chembiol.2010.07.010

9. Shen XH, Zhou NY, Liu SJ. Degradation and assimilation of aromatic compounds by Corynebacterium glutamicum: another potential for applications for this bacterium? *Appl Microbiol Biotechnol*. 2012;95(1):77-89. doi:10.1007/s00253-012-4139-4

10. Becker J, Kuhl M, Kohlstedt M, Starck S, Wittmann C. Metabolic engineering of Corynebacterium glutamicum for the production of cis, cis-muconic acid from lignin. *Microb Cell Factories*. 2018;17(1):115. doi:10.1186/s12934-018-0963-2

11. Freudl R. Beyond amino acids: Use of the Corynebacterium glutamicum cell factory for the secretion of heterologous proteins. *J Biotechnol*. 2017;258:101-109. doi:10.1016/j.jbiotec.2017.02.023

12. Gopinath V, Nampoothiri KM. Corynebacterium glutamicum. In: *Encyclopedia of Food Microbiology*. Elsevier; 2014:504-517. doi:10.1016/B978-0-12-384730-0.00076-8

13. Lee MJ, Kim P. Recombinant Protein Expression System in Corynebacterium glutamicum and Its Application. *Front Microbiol*. 2018;9:2523. doi:10.3389/fmicb.2018.02523

14. Ricklefs E, Winkler N, Koschorreck K, Urlacher VB. Expanding the laccase-toolbox: A laccase from Corynebacterium glutamicum with phenol coupling and cuprous oxidase activity. *J Biotechnol*. 2014;191:46-53. doi:10.1016/j.jbiotec.2014.05.031

15. Altschul SF, Gish W, Miller W, Myers EW, Lipman DJ. Basic local alignment search tool. *J Mol Biol*. 1990;215(3):403-410. doi:10.1016/S0022-2836(05)80360-2

16. UniProt Consortium. UniProt: the universal protein knowledgebase in 2021. *Nucleic Acids Res*. 2021;49(D1):D480-D489. doi:10.1093/nar/gkaa1100

17. Täuber S, Blöbaum L, Wendisch VF, Grünberger A. Growth Response and Recovery of Corynebacterium glutamicum Colonies on Single-Cell Level Upon Defined pH Stress Pulses. *Front Microbiol*. 2021;12:711893. doi:10.3389/fmicb.2021.711893

18. Okino S, Suda M, Fujikura K, Inui M, Yukawa H. Production of d-lactic acid by Corynebacterium glutamicum under oxygen deprivation. *Appl Microbiol Biotechnol*. 2008;78(3):449-454. doi:10.1007/s00253-007-1336-7

19. Hemmerich J, Rohe P, Kleine B, et al. Use of a Sec signal peptide library from Bacillus subtilis for the optimization of cutinase secretion in Corynebacterium glutamicum. *Microb Cell Factories*. 2016;15(1):208. doi:10.1186/s12934-016-0604-6

20. Rohe P, Venkanna D, Kleine B, Freudl R, Oldiges M. An automated workflow for enhancing microbial bioprocess optimization on a novel microbioreactor platform. *Microb Cell Factories*. 2012;11(1):144. doi:10.1186/1475-2859-11-144

21. Watanabe K, Tsuchida Y, Okibe N, et al. Scanning the Corynebacterium glutamicum R genome for high-efficiency secretion signal sequences. *Microbiology*. 2009;155(3):741-750. doi:10.1099/mic.0.024075-0

22. Yim SS, Choi JW, Lee SH, Jeong KJ. Modular Optimization of a Hemicellulose-Utilizing Pathway in *Corynebacterium glutamicum* for Consolidated Bioprocessing of Hemicellulosic Biomass. *ACS Synth Biol*. 2016;5(4):334-343. doi:10.1021/acssynbio.5b00228

23. Brockmeier U, Caspers M, Freudl R, Jockwer A, Noll T, Eggert T. Systematic Screening of All Signal Peptides from Bacillus subtilis: A Powerful Strategy in Optimizing Heterologous Protein Secretion in Gram-positive Bacteria. *J Mol Biol*. 2006;362(3):393-402. doi:10.1016/j.jmb.2006.07.034

24. van der Rest ME, Lange C, Molenaar D. A heat shock following electroporation induces highly efficient transformation of Corynebacterium glutamicum with xenogeneic plasmid DNA. *Appl Microbiol Biotechnol*. 1999;52(4):541-545. doi:10.1007/s002530051557

25. Mhatre A, Shinde S, Jha AK, et al. Corynebacterium glutamicum as an Efficient Omnivorous Microbial Host for the Bioconversion of Lignocellulosic Biomass. *Front Bioeng Biotechnol*. 2022;10:827386. doi:10.3389/fbioe.2022.827386

26. Chaudhary D, Chong F, Neupane T, Choi J, Jee JG. New Inhibitors of Laccase and Tyrosinase by Examination of Cross-Inhibition between Copper-Containing Enzymes. *Int J Mol Sci*. 2021;22(24):13661. doi:10.3390/ijms222413661

27. Lorenzo M, Moldes D, Rodríguez Couto S, Sanromán MaA. Inhibition of laccase activity from Trametes versicolor by heavy metals and organic compounds. *Chemosphere*. 2005;60(8):1124-1128. doi:10.1016/j.chemosphere.2004.12.051

28. Raseda N, Hong S, Kwon OY, Ryu K. Kinetic Evidence for the Interactive Inhibition of Laccase from Trametes versicolor by pH and Chloride. *J Microbiol Biotechnol*. 2014;24(12):1673-1678. doi:10.4014/jmb.1408.08012

29. Pamidipati S, Ahmed A. A first report on competitive inhibition of laccase enzyme by lignin degradation intermediates. *Folia Microbiol (Praha)*. 2020;65(2):431-437. doi:10.1007/s12223-019-00765-5

30. Liu H, Qi Z, Liu C. Inhibition mechanisms of humic acid and protein on the degradation of sulfamethazine by horseradish peroxidase. *Colloids Surf Physicochem Eng Asp*. 2021;629:127473. doi:10.1016/j.colsurfa.2021.127473

31. Li F, Tang Y. Inhibition mechanism: Phytic acid, NADH as a peroxidase inhibitor. *Spectrochim Acta A Mol Biomol Spectrosc*. 2021;244:118856. doi:10.1016/j.saa.2020.118856

32. Maeda T, Koch-Koerfges A, Bott M. Relevance of NADH Dehydrogenase and Alternative Two-Enzyme Systems for Growth of Corynebacterium glutamicum With Glucose, Lactate, and Acetate. *Front Bioeng Biotechnol*. 2021;8:621213. doi:10.3389/fbioe.2020.621213

33. Matsushita K, Otofuji A, Iwahashi M, Toyama H, Adachi O. NADH dehydrogenase of Corynebacterium glutamicum. Purification of an NADH dehydrogenase II homolog able to oxidize NADPH. *FEMS Microbiol Lett*. 2001;204(2):271-276. doi:10.1111/j.1574-6968.2001.tb10896.x

34. Attaallah R, Amine A. Highly selective and sensitive detection of cadmium ions by horseradish peroxidase enzyme inhibition using a colorimetric microplate reader and smartphone paper-based analytical device. *Microchem J*. 2022;172:106940. doi:10.1016/j.microc.2021.106940

35. Li F, Fu Y, Yang H, Tang Y. The inhibition mechanism of luteolin on peroxidase based on multispectroscopic techniques. *Int J Biol Macromol*. 2021;166:1072-1081. doi:10.1016/j.ijbiomac.2020.10.262

36. Babich H, Liebling EJ, Burger RF, Zuckerbraun HL, Schuck AG. Choice of DMEM, formulated with or without pyruvate, plays an important role in assessing the in vitro cytotoxicity of oxidants and prooxidant nutraceuticals. *Vitro Cell Dev Biol - Anim*. 2009;45(5-6):226-233. doi:10.1007/s11626-008-9168-z

37. Long LH, Halliwell B. Artefacts in cell culture: Pyruvate as a scavenger of hydrogen peroxide generated by ascorbate or epigallocatechin gallate in cell culture media. *Biochem Biophys Res Commun*. 2009;388(4):700-704. doi:10.1016/j.bbrc.2009.08.069

APPENDIX A

SAMPLE CALCULATIONS

Calculation of Enzyme Units

From absorbance readings in the ABTS plate assay, the Beer-Lambert law can be used to calculate the enzyme units, U, representing the amount of enzyme able to convert 1umol of ABTS in one minute. The Beer-Lambert law is given:

$$A = \varepsilon \ell c$$

where A is absorbance, ε is molar extinction coefficient (36 $mM^{-1}cm^{-1}$ for $ABTS^{\bullet+}$), ℓ is length (here 1 cm), and c is concentration. Rearranging to solve for concentration:

$$c = \frac{A}{\varepsilon \ell}$$

To look at the change in concentration over time, and therefore calculate U/L:

$$\frac{U}{L}\left[\frac{uM}{min}\right] = \frac{\Delta A}{\varepsilon \ell \Delta t}$$

Finally, to adjust for change in absorbance occurring with no enzyme, the change in absorbance of the negative control is subtracted from the experimental change in absorbance:

$$\frac{U}{L}\left[\frac{uM}{min}\right] = \frac{\Delta A_{exp} - \Delta A_{ctrl}}{\varepsilon \ell \Delta t}$$

where t is time. Utilizing real data for a sample calculation, where mean absorbance of peroxidase in water was 1.6942 at the start and 2.4788 after five minutes, and the mean for water alone at the start and after five minutes were 1.5523 and 1.5910, respectively:

$$\frac{U}{L}\left[\frac{uM}{min}\right] = \left(1000\,\frac{uM}{mM}\right)\frac{(2.4788 - 1.6942) - (1.5910 - 1.5523)}{\left(36\,\frac{1}{mM * cm}\right)(1\ cm)(5\ min)} = 4.1433\,\frac{uM}{min}$$

Error Propagation

Error for U was calculated by propagation of the error in the measurements of absorbance increase, represented by sample standard deviation. Using the equation for error propagation via addition of uncertain variables, the error can be calculated using:

$$\delta(\Delta A_{exp} - \Delta A_{ctrl}) = \sqrt{\delta\Delta A_{exp}^2 + \delta\Delta A_{ctrl}^2}$$

where δ is error. From the data, the standard deviation of the five-minute increase in absorbance was 0.0106 for peroxidase in water and 0.0093 for water alone. Substituting these values:

$$\delta(\Delta A_{exp} - \Delta A_{ctrl}) = \sqrt{0.0106^2 + 0.0093^2} = 0.0141$$

Scaling this to find the error for U:

$$\delta U = \frac{\delta(\Delta A_{exp} - \Delta A_{ctrl})}{\varepsilon \ell \Delta t} = \left(1000 \frac{uM}{mM}\right) \frac{0.0141}{\left(36 \frac{1}{mM * cm}\right)(1\ cm)(5\ min)} = 0.0783 \frac{uM}{min}$$

APPENDIX B

ADDITIONAL PICTURES OF ABTS DROP ASSAYS

ABTS drop assays with varied methods are discussed and reported in the following figures:

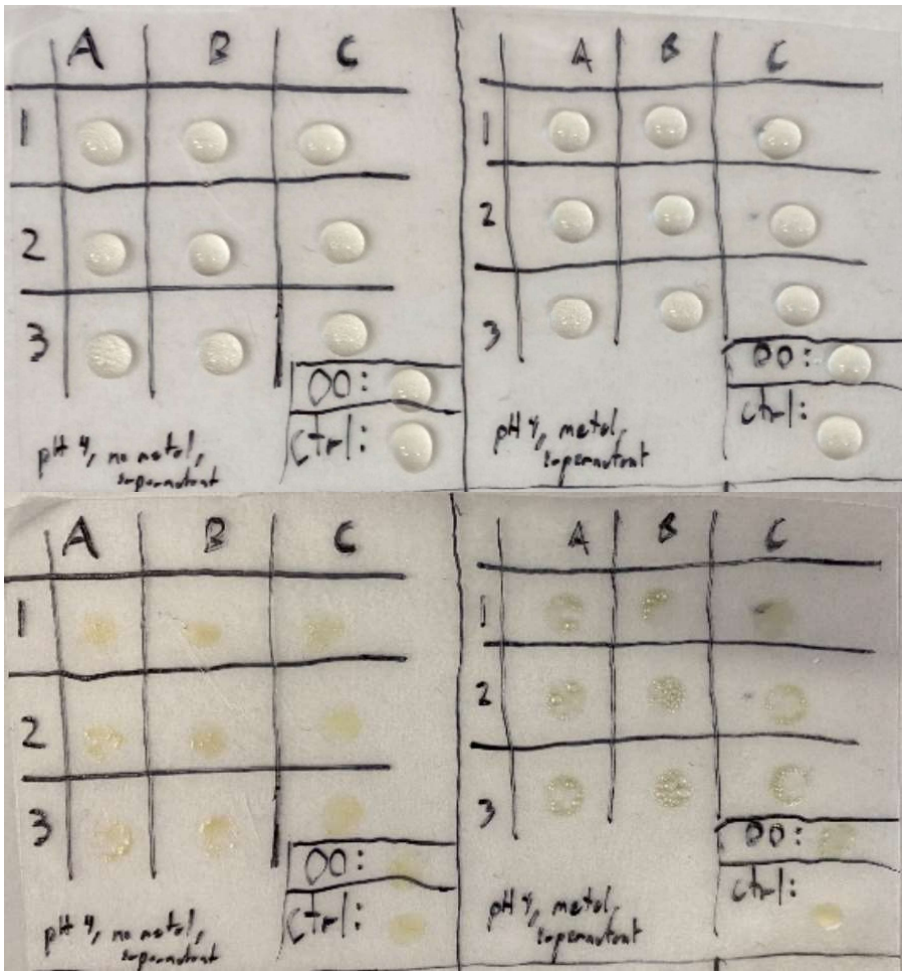

Figure B-1: ABTS drop assay experiment of all strains in BTM2 media with supplemented metals. *The top picture shows the beginning of the assay, the bottom shows the assay after being left overnight, with the drops being dried up. The left panel shows the supernatants with no metals added, whereas for the right panel 2 mM $CuSO_4$•$5H_2O$, 2 mM $FeSO_4$•$7H_2O$, and 1 mM $CaCl_2$ were added and shook (OO: control strain; ctrl: BTM2 media with no cells). For each reaction, 5 uL of 100x diluted 30% H_2O_2 was added for visualization. Dried droplets appear green for the panel with added metals, but because the control strain is also green, it is hypothesized that the metals themselves interacted with ABTS to produce the color change.*

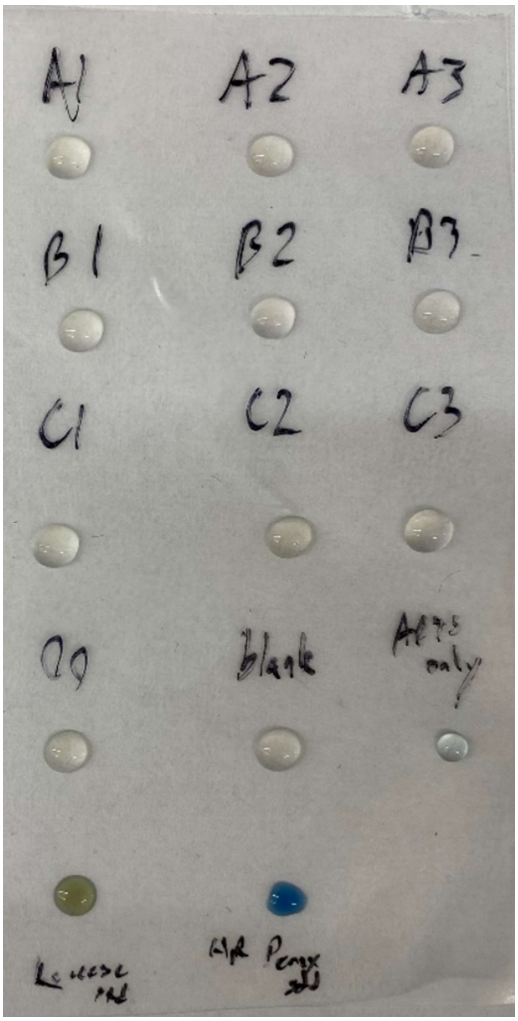

Figure B-2: ABTS drop assay of all experimental strains grown in BTM2. *Here, the drop assay for the cells with added metals from* ***Figure B-1*** *were repeated after a multi-day incubation at 4 °C with 0.5 mM ABTS used instead of 3 mM. Positive controls were also performed for comparison.*

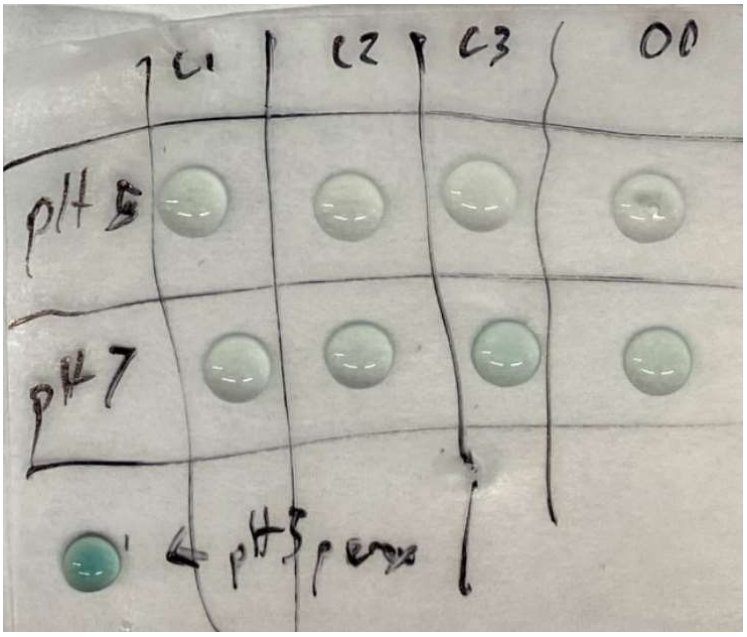

Figure B-3: ABTS drop assay of cell lysates. *The cultures from **Figure 13** were lysed after storage at 4 ºC for two days for use in this assay. To lyse the cells, 150 uL SoluLyse™ was added to the pellet of a 1 mL culture after discarding the supernatant. The pellet was then resuspended and shook for 10 minutes before again centrifuging and repeating the drop assay.*

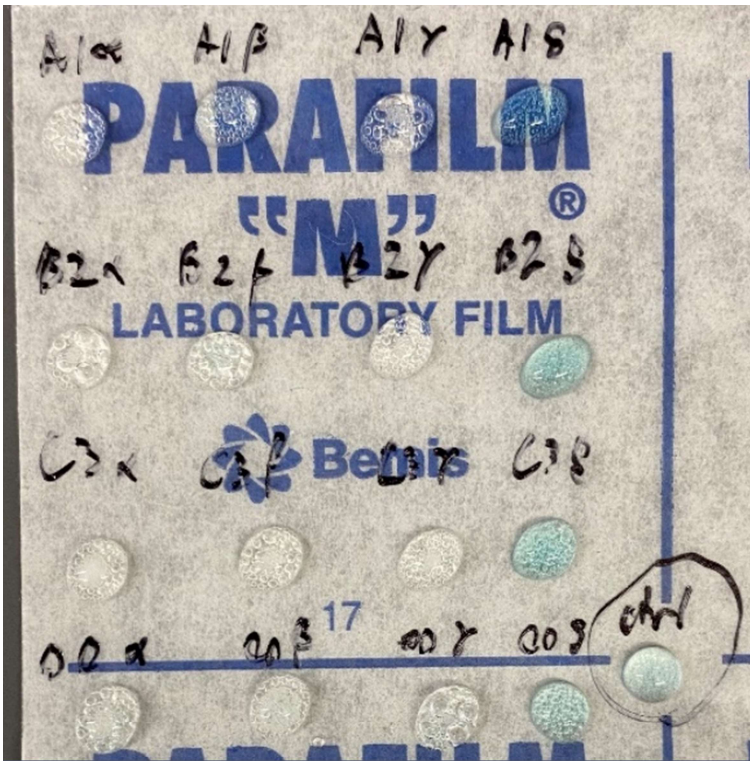

Figure B-4: ABTS drop assay experiment with select strains grown in BTM2 media with supplemented metals. *Rows are as follows: strain 'A1', 'B2', 'C3', ctrl strain ('OO'). The 'ctrl' was BTM2 media alone with ABTS. Nothing was added to the first column. At 8 hours, 0.25 mM of isopropyl β-D-1-thiogalactopyranoside (IPTG) was added to the last three columns' cultures for induction, which was unnecessary with the pCRB204-derived plasmids. At 24 hours, 0.04 mM $CuSO_4$•$5H_2O$, 0.04 mM $FeSO_4$•$7H_2O$, and 0.02 mM $CaCl_2$ were added to the third column's cultures, and 2 mM $CuSO_4$•$5H_2O$, 2 mM $FeSO_4$•$7H_2O$, and 1 mM $CaCl_2$ were added to the last column's cultures. Extra H_2O_2 was added to the reactions for visualization. No color change was observed relative to the negative control for any reaction, except for a slight green tint in the reactions in the third column. Because the control strain was also green, there is high likelihood of the metals interacting with the ABTS to cause the color change rather than the presence of lignin-modifying enzymes. Notably, the supernatants effervesced with the addition of H_2O_2*

Not pictured: plate assays were also performed and incubated at an elevated temperature of 50 ºC to enhance enzyme activity. However, immediately upon subjecting the 96-well plate to the higher temperature, the slight blue-green color of the ABTS buffer turned colorless, suggesting the ABTS could be unstable at the higher temperature.

APPENDIX C

REPLICATE FIGURES OF PEROXIDASE ABSORBANCE CURVES

Figures complementing and representing data from the other replicate from **Figure 18** are provided below.

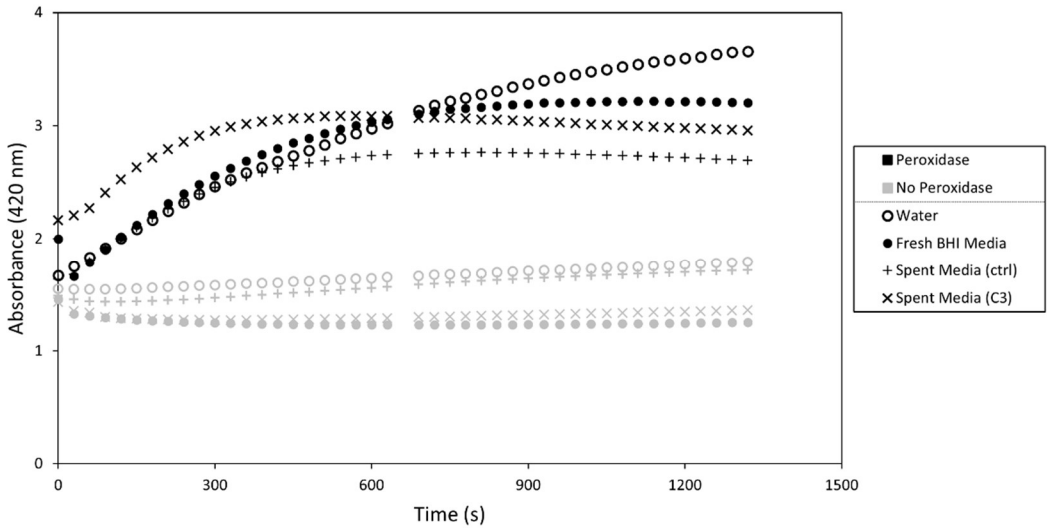

Figure C-1: Time plot of absorbance readings from the second replicate of the peroxidase positive control plate assay. *Early time point measurements of the reaction with peroxidase added in 'C3' spent media follow an odd and unexpected trajectory. The first time point measurement for the reaction with peroxidase added in fresh BHI media shows an absorbance higher and out of line with subsequent measurements.*

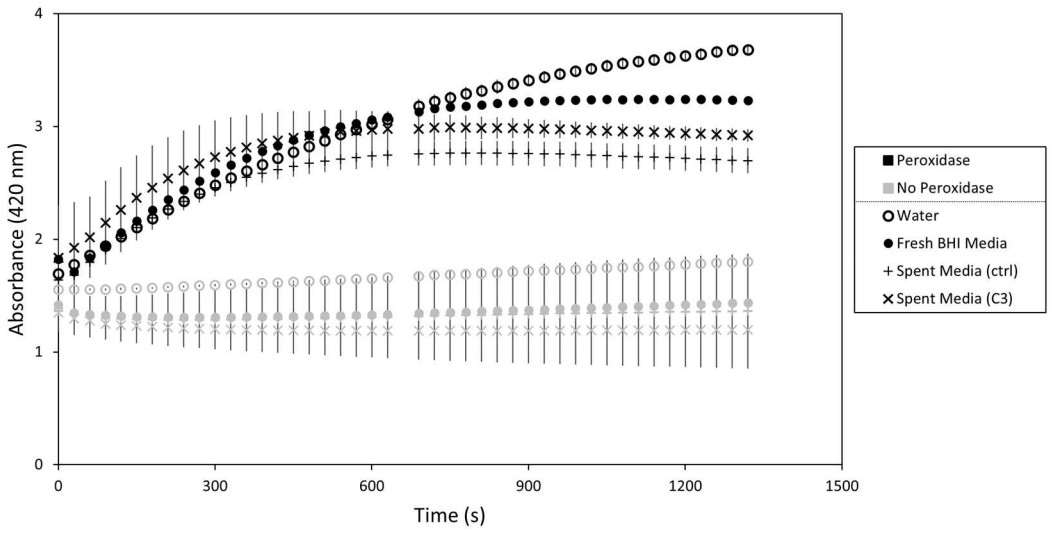

Figure C-2: Time plot of average absorbance readings from peroxidase positive control plate assay. *Error bars represent the sample standard deviation from duplicate measures. The reaction with added peroxidase in 'C3' spent media has large variance at early time points. Reactions in fresh and spent BHI with no peroxidase added also have large variance at all time points.*

APPENDIX D

UNCORRECTED ABTS ABSORBANCE DIFFERENCES

Unadjusted ABTS plate assay results for the positive peroxidase and laccase controls are presented below. Instead of subtracting the negative controls and calculating the enzyme activity (U) as in **Figures 16, 19, & 20**, here only the differences in positive control absorbances are reported and discussed.

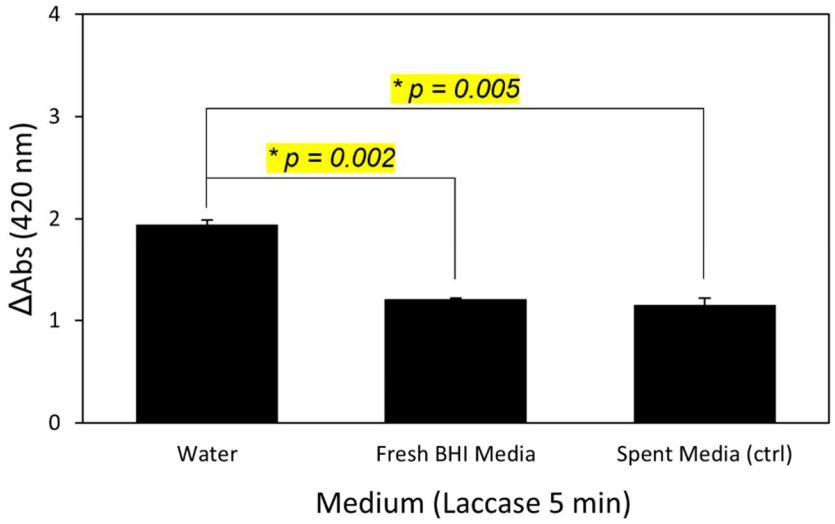

Figure D-1: Unadjusted change in ABTS absorbance via laccase reaction. *The perceived conversion of ABTS via laccase was significantly decreased when performed in BHI medium versus in water, suggesting that media components are inhibiting the reaction.*

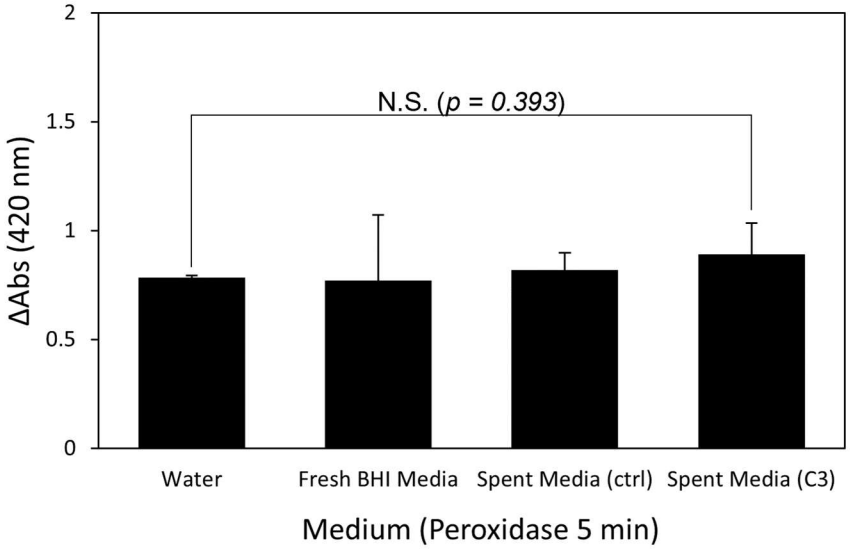

Figure D-2: Unadjusted change in ABTS absorbance via peroxidase reaction after five minutes. *When not adjusting the change in absorbance by the no-peroxidase control, there appears to be no difference in reaction at five minutes.*

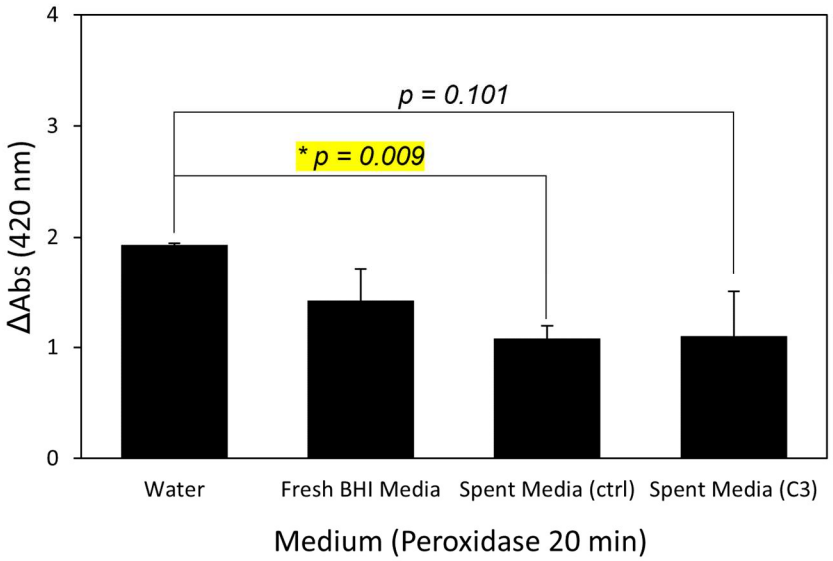

Figure D-3: Unadjusted change in ABTS absorbance via peroxidase reaction after 20 minutes. *When not adjusting the change in absorbance, the perceived conversion of ABTS is significantly decreased in spent media. This suggests the reaction may be inhibited in the supernatant, potentially by bacterial growth byproducts.*